

ISOGEOMETRIC DISCRETIZATIONS OF THE STOKES PROBLEM ON TRIMMED GEOMETRIES ^{*,**}

RICCARDO PUPPI¹

Abstract. The isogeometric approximation of the Stokes problem in a trimmed domain is studied. This setting is characterized by an underlying mesh unfitted with the boundary of the physical domain making the imposition of the essential boundary conditions a challenging problem. A very popular strategy is to rely on the so-called Nitsche method [18]. We show that the Nitsche method lacks stability in some degenerate trimmed domain configurations, potentially polluting the computed solutions. After extending the stabilization procedure of [14] to incompressible flow problems, we show that we recover the well-posedness of the formulation and, consequently, optimal a priori error estimates. Numerical experiments illustrating stability and converge rates are included.

2020 Mathematics Subject Classification. 65N12,65N30,65N85.

February 2, 2022.

INTRODUCTION

In Computer Aided Design (CAD) complex geometries are usually constructed as a set of simple spline, or more generally NURBS, geometries plus a set of Boolean operations, among which there is set difference, commonly called *trimming* in this context. Isogeometric analysis (IGA) [35] is a numerical method for approximating the solutions of PDEs to alleviate the need to remodel the geometries via a tetrahedral or hexahedral mesh, one of the major bottlenecks of the classical Finite Element Method (FEM). Following the *isoparametric paradigm* we wish to use the same basis functions employed for the parameterization of the geometric domain for the discretization and analysis of the differential problem taken into consideration. In recent years, great progress has been made in the domain of IGA to improve the usability of CAD geometries in the solution of PDEs and, in this respect, volumetric representations (V-rep) are a major contribution [2, 39]. However further efforts are needed for it to be considered a mature field. In this respect trimming is a major challenge for isogeometric methods: on one hand, it is a fundamental element in the design phase of the geometric domain, while on the other, it is an obstacle to the analysis, in particular to the development of robust and reliable solution methods. For further details about the challenges of trimming in IGA we refer the interested readers to the review article [38] and the references therein.

Keywords and phrases: isogeometric analysis, IGA, CAD, CutFEM, trimming, unfitted, Nitsche, finite element, Raviart-Thomas, Nédélec, Taylor-Hood, inf-sup, stability, stabilization

* We gratefully thank Annalisa Buffa for her teaching and advice and Rafael Vázquez Hernández for the many discussions and his precious support.

** This work was partially supported by ERC AdG project CHANGE n. 694515.

¹ Chair of Modelling and Numerical Simulation, École Polytechnique Fédérale de Lausanne, Station 8, 1015 Lausanne, Switzerland.

In practice, the simplest trimmed geometry is an object endowed with a tensor product mesh which is cut by an arbitrary line in 2D or surface in 3D. Similar challenges were considered, already long ago (see the pioneering work of Barrett and Elliott [3,4]), in the context of FEM.

Hence all the techniques developed by the finite element community come now to help. Among the most successful approaches relying on a solid mathematical foundation, there is CutFEM, a construction developed in the last decade by Burman and collaborators [16,17].

Let us outline the setting we consider in this paper. We set $\Omega_0 \subset \mathbb{R}^d$ (here $d = 2, 3$), a domain parametrized by a bijective spline map $\mathbf{F} : (0, 1)^d \rightarrow \Omega_0$, i.e., a *patch* in the isogeometric terminology, and let $\Omega_1, \dots, \Omega_N$ be Lipschitz domains in \mathbb{R}^d . We assume that Ω_i , $i = 1, \dots, N$, are to be cut away from Ω_0 and that our computational domain reads:

$$\Omega = \Omega_0 \setminus \bigcup_{i=1}^N \bar{\Omega}_i. \quad (1)$$

In this paper, we contribute to the development of robust isogeometric numerical methods for PDEs in a trimmed domain such as (1). It is known that the main sources of issues are: integration, conditioning, and stability [14]. Here, we address the stability of incompressible flow problems in trimmed geometries. For what concerns integration, namely the construction of suitable quadrature rules on the cut elements, we rely on the technique developed in [2]. The conditioning issue is also out of the scope of this work: herein we limit ourselves to applying a block diagonal rescaling of the basis functions. Our contribution lies on the theoretical side and extends the analysis developed in [14] to incompressible flow problems. We introduce the Raviart-Thomas, Nédélec, and Taylor-Hood mixed isogeometric elements (first studied in [13]) and adapt their definitions to trimmed domains. For the weak imposition of the Dirichlet boundary conditions, we rely on Nitsche’s method. After empirically demonstrating the lack of stability of the Nitsche formulation, we propose our stabilization. On the one hand, just as in the elliptic case, we modify the evaluation of the normal derivatives of the velocities at the “badly” cut elements. At the same time, we apply the stabilization to the whole space of pressures, by substituting the degrees of freedom (DOFs) at the bad elements with a linear combination from a “good” neighboring element. Let us observe that a mathematical proof of the inf-sup condition for the stabilized formulation is still missing. However, numerical experiments indicate that our approach works.

Let us now briefly review the literature about isogeometric methods on trimmed domains. First of all, we observe that most of the contributions to this topic propose to weakly enforce Dirichlet boundary conditions using the Nitsche method [46] and they adopt the adaptive quadrature strategy developed in [43]. For instance, let us refer to the papers in immersogeometric methods for fluid-structure interactions [36,37] where the structure is immersed in the background mesh of the fluid which is cut in an arbitrary fashion. In a series of articles [32–34] Hoang et al. employ different families of stable (in the boundary fitted case) isogeometric elements, namely the Taylor-Hood element [7, 11–13], the Raviart-Thomas element [13, 15, 23], the Nédélec element [13] and the Subgrid element [12], and empirically show that the well-posedness and good conditioning in the unfitted case can be recovered by adding to the variational formulation a consistent term penalizing the jumps of high-order derivatives of the pressure, in the spirit of [8, 18]. In [21] the authors develop an overlapping Additive-Schwarz preconditioner tailored for incompressible flow problems, without addressing the stability issue.

The manuscript is structured as follows. After having introduced in Section 1 some notations and the strong formulation of the Stokes problem, in Section 2 we provide the basic notions on IGA: we introduce three families of isogeometric elements (Raviart-Thomas, Nédélec, and Taylor-Hood) and use them to discretize the considered equations using Nitsche’s method for the imposition of the essential boundary conditions. In Section 3 we show through numerical experiments that the Nitsche formulation is not stable for the trimming operation. Then, in Section 4 we introduce our stabilized Nitsche formulation and then move on to its numerical analysis in Section 5. We demonstrate that the stabilized formulation is well-posed and, in Section 6, that we have optimal a priori error estimates. In Section 7 we provide several numerical experiments to validate the effectiveness of our stabilization procedure.

1. NOTATION AND MODEL PROBLEM

We briefly introduce some useful notations for the forthcoming analysis. Let D be a Lipschitz-regular *domain* (subset, open, bounded, connected) of \mathbb{R}^d , $d \in \{2, 3\}$. Let $L^2(D)$ denote the space of square integrable functions on D , equipped with the usual norm $\|\cdot\|_{L^2(D)}$. Let $L_0^2(D)$ be the subspace of $L^2(D)$ of functions with zero average. We denote by $H^n(D)$, for $n \in \mathbb{N}$, the standard Sobolev space of functions in $L^2(D)$ whose n -th order weak derivatives belong to $L^2(D)$. We define, for $\varphi : D \rightarrow \mathbb{R}$ sufficiently regular and $\boldsymbol{\eta}$ multi-index with $|\boldsymbol{\eta}| := \sum_{i=1}^d \eta_i$, $D^{\boldsymbol{\eta}}\varphi := \frac{\partial^{|\boldsymbol{\eta}}\varphi}{\partial x_1^{\eta_1} \dots \partial x_d^{\eta_d}}$, $\|\varphi\|_{H^n(D)}^2 := \sum_{|\boldsymbol{\eta}| \leq n} \|D^{\boldsymbol{\eta}}\varphi\|_{L^2(D)}^2$. Sobolev spaces of fractional order $H^k(D)$, $k \in \mathbb{R}$, can be defined by interpolation techniques, see [1]. Let us denote $\mathbf{L}^2(D) := (L^2(D))^d$ and $\mathbf{H}^k(D) := (H^k(D))^d$. We define the Hilbert space $\mathbf{H}(\text{div}; D)$ of vector fields in $\mathbf{L}^2(D)$ with divergence in $L^2(D)$, endowed with the graph norm $\|\cdot\|_{\mathbf{H}(\text{div}; D)}$. Let $H^{\frac{1}{2}}(\partial D)$ be the range of the trace operator of functions in $H^1(D)$ and, for a non-empty open subset of the boundary ω , we define its restriction $H^{\frac{1}{2}}(\omega)$. Both $H^{\frac{1}{2}}(\partial D)$ and $H^{\frac{1}{2}}(\omega)$ can be endowed with an intrinsic norm, see [48]. The dual space of $H^{\frac{1}{2}}(\omega)$ is denoted $H^{-\frac{1}{2}}(\omega)$. Finally, let $\mathbf{H}^{\frac{1}{2}}(\partial D) := \left(H^{\frac{1}{2}}(\partial D)\right)^d$, $\mathbf{H}^{\frac{1}{2}}(\omega) := \left(H^{\frac{1}{2}}(\omega)\right)^d$ and $\mathbf{H}^{-\frac{1}{2}}(\omega) := \left(H^{-\frac{1}{2}}(\omega)\right)^d$.

For the sake of convenience, we are going to employ the same notation $|\cdot|$ for the volume (Lebesgue), the surface (Hausdorff) measures of \mathbb{R}^d and the cardinality of a set. We also denote as $\mathbb{Q}_{r,s,t}$ the vector space of polynomials of degree at most r in the first variable, at most s in the second and at most t in the third one (analogously for the case $d = 2$), \mathbb{P}_u the vector space of polynomials of degree at most u . We may write \mathbb{Q}_k instead of $\mathbb{Q}_{k,k}$ or $\mathbb{Q}_{k,k,k}$. Given $E \subset \mathbb{R}^d$, the notation $\text{int } E$ denote its interior.

Let us assume Ω to be a Lipschitz domain obtained via trimming operations, as in (1) with $N = 1$, namely $\Omega = \Omega_0 \setminus \overline{\Omega}_1$. Let Γ be its boundary such that $\Gamma = \overline{\Gamma}_D \cup \overline{\Gamma}_N$, where Γ_D and Γ_N are non-empty, open, and disjoint. We denote the *trimming curve* (respectively surface if $d = 3$) as $\Gamma_T = \Gamma \cap \partial\Omega_1$.

Note that throughout this document C will denote generic constants that may change at each occurrence, but that are always independent of the local mesh size and on the way the background mesh is cut by the trimming curve, unless otherwise specified. The equivalence $cx \leq y \leq Cx$ is denoted by $x \sim y$.

The Stokes equations are a linear system that can be derived as a simplification of the Navier-Stokes equations. They describe the flow of a fluid under incompressibility and slow motion regimes. Given the body force $\mathbf{f} : \Omega \rightarrow \mathbb{R}^d$, the mass production rate $g : \Omega \rightarrow \mathbb{R}$, the Dirichlet datum $\mathbf{u}_D : \Omega \rightarrow \mathbb{R}$ and the Neumann datum $\boldsymbol{\sigma}_N : \Omega \rightarrow \mathbb{R}$, we look for the *velocity* $\mathbf{u} : \Omega \rightarrow \mathbb{R}^d$ and *pressure* $p : \Omega \rightarrow \mathbb{R}$ such that

$$\begin{aligned}
 -\text{div } \boldsymbol{\sigma}(\mathbf{u}, p) &= \mathbf{f}, & \text{in } \Omega, \\
 \text{div } \mathbf{u} &= g, & \text{in } \Omega, \\
 \mathbf{u} &= \mathbf{u}_D, & \text{on } \Gamma_D, \\
 \boldsymbol{\sigma}(\mathbf{u}, p)\mathbf{n} &= \boldsymbol{\sigma}_N, & \text{on } \Gamma_N,
 \end{aligned} \tag{2}$$

where $\mu \in \mathbb{R}$, $\mu > 0$ is the *viscosity coefficient*, $\boldsymbol{\sigma}(\mathbf{u}, p) = \mu D\mathbf{u} - p\mathbf{I}$ is the *Cauchy stress tensor*. The first equation is known as the *conservation of the momentum* and is nothing else than the Newton's Second Law, relating the external forces acting on the fluid to the rate of change of its momentum, the second one is the *conservation of mass* (when $g \equiv 0$). In what follows, we assume $\mu \equiv 1$ for the sake of simplicity of the notation.

2. THE ISOGEOMETRIC DISCRETIZATION

2.1. Univariate B-splines

For a more detailed introduction to isogeometric analysis, we refer the interested reader to the review article [9]. Given two positive integers k and n , we say that $\Xi := \{\xi_1, \dots, \xi_{n+k+1}\}$ is a k -open knot vector if

$$\xi_1 = \dots = \xi_{k+1} < \xi_{k+2} \leq \dots \leq \xi_n < \xi_{n+1} = \dots = \xi_{n+k+1}.$$

We assume $\xi_1 = 0$ and $\xi_{n+k+1} = 1$. We also introduce $Z := \{\zeta_1, \dots, \zeta_M\}$, the set of *breakpoints*, or knots without repetitions, which forms a partition of the interval $(0, 1)$. Note that

$$\Xi = \underbrace{\{\zeta_1, \dots, \zeta_1\}}_{m_1 \text{ times}}, \underbrace{\{\zeta_2, \dots, \zeta_2\}}_{m_2 \text{ times}}, \dots, \underbrace{\{\zeta_M, \dots, \zeta_M\}}_{m_M \text{ times}},$$

where m_j is the multiplicity of the breakpoint ζ_j and $\sum_{i=1}^M m_i = n + k + 1$. Moreover, we assume $m_j \leq k$ for every internal knot and we denote $I_i := (\zeta_i, \zeta_{i+1})$ and its measure $h_i := \zeta_{i+1} - \zeta_i$, $i = 1, \dots, M - 1$.

We denote as $\widehat{B}_{i,k} : [0, 1] \rightarrow \mathbb{R}$ the i -th B -spline of degree k , $1 \leq i \leq n$, obtained using the *Cox-de Boor formula*, see for instance [9]. Moreover, let $S_{\alpha}^k(\Xi) := \text{span}\{\widehat{B}_{i,k} : 1 \leq i \leq n\}$ be the vector space of univariate splines of degree k , which can also be characterized as the space of piecewise polynomials of degree k with $\alpha_j := k - m_j$ continuous derivatives at the breakpoints ζ_j , $1 \leq j \leq M$ (the *Curry-Schoenberg Theorem*). The number of continuous derivatives at the breakpoints are collected in the *regularity vector* $\alpha := (\alpha_j)_{j=1}^M$. A knot multiplicity $m_j = k + 1$ corresponds to a regularity $\alpha_j = -1$, *i.e.*, a discontinuity at the breakpoint ζ_j . Since the knot vector is open, it holds $\alpha_1 = \alpha_M = -1$. For the sake of simplicity of the notation we assume that the basis functions have the same regularity at the internal knots, namely $\alpha_j = \alpha$ for $2 \leq j \leq M - 1$. Moreover, given an interval $I_j = (\zeta_j, \zeta_{j+1}) = (\xi_i, \xi_{i+1})$, we define its *support extension* \widetilde{I}_j as

$$\widetilde{I}_j := \text{int} \bigcup \{ \text{supp}(\widehat{B}_{\ell,k}) : \text{supp}(\widehat{B}_{\ell,k}) \cap I_j \neq \emptyset, 1 \leq \ell \leq n \} = (\xi_{i-k}, \xi_{i+k+1}).$$

2.2. Multivariate B-splines

Let $d \in \{2, 3\}$ denote the space dimension and $M_{\ell}, n_{\ell}, k_{\ell} \in \mathbb{N}$, $\Xi_{\ell} = \{\xi_{\ell,1}, \dots, \xi_{\ell, n_{\ell} + k_{\ell} + 1}\}$, $Z_{\ell} = \{\zeta_{\ell,1}, \dots, \zeta_{\ell, M_{\ell}}\}$ be given, for every $1 \leq \ell \leq d$. We set the degree vector $\mathbf{k} := (k_1, \dots, k_d)$, the regularity vectors α_{ℓ} , $1 \leq \ell \leq d$, and the multivariate knot-vector $\Xi := \Xi_1 \times \dots \times \Xi_d$. As in the univariate case, we assume that the same regularity holds at the internal knots for every parametric direction, hence we drop the bold font once for all and write α_{ℓ} , $1 \leq \ell \leq d$. Note that the breakpoints of Z_{ℓ} form a Cartesian grid in the parametric domain $\widehat{\Omega}_0 := (0, 1)^d$, namely the *parametric Bézier mesh*

$$\widehat{\mathcal{M}}_{0,h} = \{Q_{\mathbf{j}} = I_{1,j_1} \times \dots \times I_{d,j_d} : I_{\ell,j_{\ell}} = (\zeta_{\ell,j_{\ell}}, \zeta_{\ell,j_{\ell}+1}) : 1 \leq j_{\ell} \leq M_{\ell} - 1\},$$

where each $Q_{\mathbf{j}}$ is called *parametric Bézier element*, with $h_{Q_{\mathbf{j}}} := \text{diam}(Q_{\mathbf{j}})$. We require the following hypothesis that allows us to assign h_Q as a unique measure to each element and to use the Bramble-Hilbert type results developed in [7].

Assumption 2.1. The family of meshes $\{\widehat{\mathcal{M}}_{0,h}\}_h$ is assumed to be *shape-regular*, that is, the ratio between the smallest edge of $Q \in \widehat{\mathcal{M}}_{0,h}$ and its diameter h_Q is uniformly bounded with respect to Q and h .

Remark 2.2. The shape-regularity hypothesis implies that the mesh is *locally-quasi uniform*, *i.e.*, the ratio of the sizes of two neighboring elements is uniformly bounded (see [7]).

Let $\mathbf{I} := \{\mathbf{i} = (i_1, \dots, i_d) : 1 \leq i_{\ell} \leq n_{\ell}\}$ be a set of multi-indices. For each $\mathbf{i} = (i_1, \dots, i_d)$, we define the set of *multivariate B-splines* $\{\widehat{B}_{\mathbf{i},\mathbf{k}}(\zeta) = \widehat{B}_{i_1,k_1}(\zeta_1) \dots \widehat{B}_{i_d,k_d}(\zeta_d) : \mathbf{i} \in \mathbf{I}\}$. Moreover, for a generic Bézier

element $Q_j \in \widehat{\mathcal{M}}_{0,h}$, we define its *support extension* $\widetilde{Q}_j = \widetilde{I}_{1,j_1} \times \cdots \times \widetilde{I}_{d,j_d}$, where $\widetilde{I}_{\ell,j_\ell}$ is the univariate support extension of the univariate case defined above. The *multivariate spline space* in $\widehat{\Omega}_0$ is defined as $S_{\alpha_1, \dots, \alpha_d}^{\mathbf{k}}(\Xi) = \text{span}\{\widehat{B}_{\mathbf{i},\mathbf{k}}(\zeta) : \mathbf{i} \in \mathbf{I}\}$, which can also be seen as the space of piecewise multivariate polynomials of degree \mathbf{k} and with regularity across the internal Bézier elements given by $\alpha_1, \dots, \alpha_d$. Note that $S_{\alpha_1, \dots, \alpha_d}^{\mathbf{k}}(\Xi) = S_{\alpha_1, \dots, \alpha_d}^{\mathbf{k}}(\Xi_1, \dots, \Xi_d) = \bigotimes_{i=1}^d S_{\alpha_i}^{k_i}(\Xi_i)$.

Remark 2.3. What has been said so far can be easily generalized to the case of Non-Uniform Rational B-Splines (NURBS) basis functions. See, for instance, [19].

2.3. Isogeometric spaces for the Stokes problem on trimmed geometries

As already said in the introduction, the principle of isogeometric methods is to assume the physical untrimmed domain Ω_0 to be the image of the unit d -dimensional cube through $\mathbf{F} \in (S_{\alpha_1, \dots, \alpha_d}^{\mathbf{k}}(\Xi))^d$, namely $\Omega_0 = \mathbf{F}(\widehat{\Omega}_0)$. Note that the *isogeometric map* \mathbf{F} is given from the CAD description of the geometry. We define the *physical Bézier mesh* as the image of the elements in $\widehat{\mathcal{M}}_{0,h}$ through \mathbf{F} , $\mathcal{M}_{0,h} := \{K : K = \mathbf{F}(Q), Q \in \widehat{\mathcal{M}}_{0,h}\}$. We denote $h_K := \text{diam}(K)$, and the support extension $\widetilde{K} := \mathbf{F}(\widetilde{Q})$, for each $K \in \mathcal{M}_{0,h}$ such that $K = \mathbf{F}(Q)$. To prevent the existence of singularities in the parametrization we make the following assumption.

Assumption 2.4. The parametrization $\mathbf{F} : \widehat{\Omega}_0 \rightarrow \Omega_0$ is bi-Lipschitz. Moreover, $\mathbf{F}|_{\overline{Q}} \in C^\infty(\overline{Q})$, for every $Q \in \widehat{\mathcal{M}}_{0,h}$, and $\mathbf{F}^{-1}|_{\overline{K}} \in C^\infty(\overline{K})$, for every $K \in \mathcal{M}_{0,h}$.

Some consequences of Assumption 2.4 are the following.

- (1) $h_Q \approx h_K$, i.e., there exist $C_1 > 0, C_2 > 0$ such that $C_1 h_K \leq h_Q \leq C_2 h_K$, for every $K \in \mathcal{M}_{0,h}$, $Q \in \widehat{\mathcal{M}}_{0,h}$, $K = \mathbf{F}(Q)$.
- (2) There exists $C > 0$ such that, for every $Q \in \widehat{\mathcal{M}}_{0,h}$ such that $\mathbf{F}(Q) = K$, it holds $\|\mathbf{DF}\|_{L^\infty(Q)} \leq C$ and $\|\mathbf{DF}^{-1}\|_{L^\infty(K)} \leq C$.
- (3) There exist $C_1 > 0, C_2 > 0$ such that, for every $\zeta \in \widehat{\Omega}_0$, $C_1 \leq |\det(\mathbf{DF}(\zeta))| \leq C_2$.

Moreover, note that Assumption 2.4 implies that if the parametric mesh is shape-regular, then the physical mesh is shape-regular too. With an abuse of notation, we may denote $h := \max_{K \in \mathcal{M}_{0,h}} h_K$, even if the same symbol has been used for the maximum diameter of the parametric mesh.

To define the isogeometric spaces in the parametric domain, we need to resort to the following cumbersome notation. For every $1 \leq \ell \leq d$, let Ξ_ℓ be a knot vector of degree k and regularity vector α , with $\Xi = \Xi_1 \times \cdots \times \Xi_\ell$ is the knot vector used for the geometry. We construct $\check{\Xi}_\ell$, a knot vector of degree $k+1$ and regularity $\alpha+1$, from Ξ_ℓ by adding one repetition of the first and last knots. By increasing the multiplicity of the internal knots $\check{\Xi}_\ell$ by one, we obtain $\widetilde{\Xi}_\ell$, a knot vector of degree $k+1$ and regularity α .

$$\begin{aligned} \widehat{V}_{0,h}^{\text{RT}} &:= \begin{cases} S_{\alpha+1,\alpha}^{k+1,k}(\check{\Xi}_1, \Xi_2) \times S_{\alpha,\alpha+1}^{k,k+1}(\Xi_1, \check{\Xi}_2), & \text{if } d = 2, \\ S_{\alpha+1,\alpha,\alpha}^{k+1,k,k}(\check{\Xi}_1, \Xi_2, \Xi_3) \times S_{\alpha,\alpha+1,\alpha}^{k,k+1,k}(\Xi_1, \check{\Xi}_2, \Xi_3) \times S_{\alpha,\alpha,\alpha+1}^{k,k,k+1}(\Xi_1, \Xi_2, \check{\Xi}_3), & \text{if } d = 3, \end{cases} \\ \widehat{V}_{0,h}^{\text{N}} &:= \begin{cases} S_{\alpha+1,\alpha}^{k+1,k+1}(\check{\Xi}_1, \widetilde{\Xi}_2) \times S_{\alpha,\alpha+1}^{k+1,k+1}(\widetilde{\Xi}_1, \check{\Xi}_2), & \text{if } d = 2, \\ S_{\alpha+1,\alpha,\alpha}^{k+1,k+1,k+1}(\check{\Xi}_1, \widetilde{\Xi}_2, \widetilde{\Xi}_3) \times S_{\alpha,\alpha+1,\alpha}^{k+1,k+1,k+1}(\widetilde{\Xi}_1, \check{\Xi}_2, \widetilde{\Xi}_3) \times S_{\alpha,\alpha,\alpha+1}^{k+1,k+1,k+1}(\widetilde{\Xi}_1, \widetilde{\Xi}_2, \check{\Xi}_3), & \text{if } d = 3, \end{cases} \\ \widehat{V}_{0,h}^{\text{TH}} &:= \begin{cases} S_{\alpha,\alpha}^{k+1,k+1}(\widetilde{\Xi}_1, \widetilde{\Xi}_2) \times S_{\alpha,\alpha}^{k+1,k+1}(\widetilde{\Xi}_1, \widetilde{\Xi}_2), & \text{if } d = 2, \\ S_{\alpha,\alpha,\alpha}^{k+1,k+1,k+1}(\widetilde{\Xi}_1, \widetilde{\Xi}_2, \widetilde{\Xi}_3) \times S_{\alpha,\alpha,\alpha}^{k+1,k+1,k+1}(\widetilde{\Xi}_1, \widetilde{\Xi}_2, \widetilde{\Xi}_3) \times S_{\alpha,\alpha,\alpha}^{k+1,k+1,k+1}(\widetilde{\Xi}_1, \widetilde{\Xi}_2, \widetilde{\Xi}_3), & \text{if } d = 3, \end{cases} \\ \widehat{Q}_{0,h} &:= \begin{cases} S_{\alpha,\alpha}^{k,k}(\Xi_1, \Xi_2), & \text{if } d = 2, \\ S_{\alpha,\alpha,\alpha}^{k,k,k}(\Xi_1, \Xi_2, \Xi_3), & \text{if } d = 3. \end{cases} \end{aligned}$$

It holds $\widehat{V}_h^{\text{RT}} \subset \widehat{V}_h^{\text{N}} \subset \widehat{V}_h^{\text{TH}}$, see [13].

We observe that the previous construction as well as what follows could be done in a more general setting, by considering different degrees and regularities for each parametric direction. We also note that, for $\alpha = -1$, $\widehat{V}_h^{\text{RT}}$ and \widehat{V}_h^{N} recover the classical Raviart-Thomas finite element and Nédélec finite element of the second kind, respectively. For $\alpha = 0$, $\widehat{V}_h^{\text{TH}}$ represents the classical Taylor-Hood finite element space. Henceforth we assume $\alpha \geq 0$, otherwise \widehat{V}_h^\square , $\square \in \{\text{RT}, \text{N}, \text{TH}\}$, is a discontinuous space (of *jump type*) and it does not provide a suitable discretization for the velocity solution of the Stokes problem, since it is not \mathbf{H}^1 -conforming.

The isogeometric spaces in the untrimmed domain Ω_0 read as follows:

$$\begin{aligned} V_{0,h}^{\text{RT}} &:= \{\mathbf{v}_h : \iota_v(\mathbf{v}_h) \in \widehat{V}_{0,h}^{\text{RT}}\}, \quad V_{0,h}^{\text{N}} := \{\mathbf{v}_h : \iota_v(\mathbf{v}_h) \in \widehat{V}_{0,h}^{\text{N}}\}, \quad V_{0,h}^{\text{TH}} := \{\mathbf{v}_h : \mathbf{v}_h \circ \mathbf{F} \in \widehat{V}_{0,h}^{\text{TH}}\}, \\ Q_{0,h}^{\text{RT}} = Q_{0,h}^{\text{N}} &:= \{q_h : \iota_p(q_h) \in \widehat{Q}_{0,h}\}, \quad Q_{0,h}^{\text{TH}} := \{q_h : q_h \circ \mathbf{F} \in \widehat{Q}_{0,h}\}, \end{aligned}$$

where ι_v and ι_p are, respectively, the divergence-preserving and integral-preserving transformations, defined as

$$\begin{aligned} \iota_v : \mathbf{H}(\text{div}; \Omega_0) &\rightarrow \mathbf{H}(\text{div}; \widehat{\Omega}_0), & \iota_v(\mathbf{v}) &:= \det(D\mathbf{F}) D\mathbf{F}^{-1}(\mathbf{v} \circ \mathbf{F}), \\ \iota_p : L^2(\Omega_0) &\rightarrow L^2(\widehat{\Omega}_0), & \iota_p(q) &:= \det(D\mathbf{F})(q \circ \mathbf{F}). \end{aligned}$$

Let us restrict them to the the active part of the domain, *i.e.*,

$$\begin{aligned} V_h^{\text{RT}} &:= \{\mathbf{v}_h|_\Omega : \mathbf{v}_h \in V_{0,h}^{\text{RT}}\}, \quad V_h^{\text{N}} := \{\mathbf{v}_h|_\Omega : \mathbf{v}_h \in V_{0,h}^{\text{N}}\}, \quad V_h^{\text{TH}} := \{\mathbf{v}_h|_\Omega : \mathbf{v}_h \in V_{0,h}^{\text{TH}}\}, \\ Q_h^{\text{RT}} = Q_h^{\text{N}} &:= \{q_h|_\Omega : q_h \in Q_{0,h}^{\text{RT}}\}, \quad Q_h^{\text{TH}} := \{q_h|_\Omega : q_h \in Q_{0,h}^{\text{TH}}\}. \end{aligned}$$

We observe that in general, in the physical domain, $V_h^{\text{RT}} \subset V_h^{\text{N}} \not\subset V_h^{\text{TH}}$.

To alleviate the notation, we may omit the superscript $\square \in \{\text{RT}, \text{N}, \text{TH}\}$ when what said does not depend from the particular isogeometric element choice.

It will be convenient to define the *active parametric Bézier mesh* $\widehat{\mathcal{M}}_h = \{Q \in \widehat{\mathcal{M}}_{0,h} : Q \cap \widehat{\Omega} \neq \emptyset\}$, where $\widehat{\Omega} = \mathbf{F}^{-1}(\Omega)$, and, similarly, the *active physical Bézier mesh* $\mathcal{M}_h = \{K : K = \mathbf{F}(Q), Q \in \widehat{\mathcal{M}}_h\}$. For every $K \in \mathcal{M}_h$, let $h_K := \text{diam}(K)$ and $h := \max_{K \in \mathcal{M}_h} h_K$. We define $\mathbf{h} : \Omega \rightarrow (0, +\infty)$ to be the piecewise constant mesh-size function of \mathcal{M}_h , assigning to the active part of each element $K \in \mathcal{M}_h$ its whole diameter, namely $\mathbf{h}|_{K \cap \Omega} := h_K$. The elements whose interiors are cut by the trimming curve (or surface) are denoted as \mathcal{G}_h , namely, $\mathcal{G}_h := \{K \in \mathcal{M}_h : \Gamma_K \neq \emptyset\}$, where $\Gamma_K := \Gamma \cap K$.

The following result holds since Γ is assumed to be Lipschitz-regular, hence not too oscillating.

Lemma 2.5. *There exists $C > 0$ such that, for every $K \in \mathcal{G}_h$, it holds $|\Gamma_K| \leq Ch_K^{d-1}$.*

Proof. See [25]. □

We endow the discrete spaces of the velocities with the scalar product

$$(\mathbf{w}_h, \mathbf{v}_h)_{1,h} := \int_\Omega D\mathbf{w}_h : D\mathbf{v}_h + \int_{\Gamma_D} \mathbf{h}^{-1} \mathbf{w}_h \cdot \mathbf{v}_h, \quad \mathbf{w}_h, \mathbf{v}_h \in V_h,$$

inducing the mesh-dependent norm

$$\|\mathbf{v}_h\|_{1,h}^2 := \|D\mathbf{v}_h\|_{L^2(\Omega)}^2 + \left\| \mathbf{h}^{-\frac{1}{2}} \mathbf{v}_h \right\|_{L^2(\Gamma_D)}^2, \quad \mathbf{v}_h \in V_h.$$

We also equip the discrete spaces of the pressures with the mesh-dependent norm

$$\|q_h\|_{0,h}^2 := \|q_h\|_{L^2(\Omega)}^2 + \left\| \mathbf{h}^{\frac{1}{2}} q_h \right\|_{L^2(\Gamma_D)}^2, \quad q_h \in Q_h.$$

We consider the following *Nitsche's formulations* as discretizations of problem (2).

Find $(\mathbf{u}_h, p_h) \in V_h \times Q_h$ such that

$$\begin{aligned} a_h(\mathbf{u}_h, \mathbf{v}_h) + b_1(\mathbf{v}_h, p_h) &= F_h(\mathbf{v}_h), & \forall \mathbf{v}_h \in V_h, \\ b_m(\mathbf{u}_h, q_h) &= G_m(q_h), & \forall q_h \in Q_h, \end{aligned} \quad (3)$$

where $m \in \{0, 1\}$ and

$$\begin{aligned} a_h(\mathbf{w}_h, \mathbf{v}_h) &:= \int_{\Omega} D\mathbf{w}_h : D\mathbf{v}_h - \int_{\Gamma_D} D\mathbf{w}_h \mathbf{n} \cdot \mathbf{v}_h - \int_{\Gamma_D} \mathbf{w}_h \cdot D\mathbf{v}_h \mathbf{n} \\ &\quad + \gamma \int_{\Gamma_D} \mathbf{h}^{-1} \mathbf{w}_h \cdot \mathbf{v}_h, & \mathbf{w}_h, \mathbf{v}_h \in V_h, \\ b_m(\mathbf{v}_h, q_h) &:= - \int_{\Omega} q_h \operatorname{div} \mathbf{v}_h + m \int_{\Gamma_D} q_h \mathbf{v}_h \cdot \mathbf{n}, & \mathbf{v}_h \in V_h, q_h \in Q_h, \\ F_h(\mathbf{v}_h) &:= \int_{\Omega} \mathbf{f} \cdot \mathbf{v}_h + \int_{\Gamma_N} \mathbf{u}_N \cdot \mathbf{v}_h - \int_{\Gamma_D} \mathbf{u}_D \cdot D\mathbf{v}_h \mathbf{n} + \gamma \int_{\Gamma_D} \mathbf{h}^{-1} \mathbf{u}_D \cdot \mathbf{v}_h, & \mathbf{v}_h \in V_h, \\ G_m(q_h) &:= - \int_{\Omega} g q_h + m \int_{\Gamma_D} q_h \mathbf{u}_D \cdot \mathbf{n}, & q_h \in Q_h, \end{aligned}$$

$\gamma > 0$ being a penalty parameter.

Remark 2.6. In the literature, the Nitsche formulation of the Stokes problem was introduced in [26] with $m = 1$ and allows to weakly impose the Dirichlet boundary conditions without manipulating the discrete velocity space. The choice $m = 0$ allows for an exactly divergence-free numerical solution for the velocity field in the case of $g \equiv 0$ and the Raviart-Thomas isogeometric element, see Remark 4.10.

Remark 2.7. We observe that, in order to simplify the presentation, in formulation (3) we impose Dirichlet conditions weakly everywhere. In the case where there is $\tilde{\Gamma} \subset \Gamma_D$ such that $\mathbf{F}^{-1}(\tilde{\Gamma})$ is a union of full faces of $\hat{\Omega}_0$, then one could have strongly imposed Dirichlet's conditions on $\tilde{\Gamma}$ by appropriately modifying the discrete velocity spaces: the traces for V_h^{TH} and the normal components for V_h^{RT} and V_h^{N} (the tangential components are weakly imposed in the spirit of [24]).

Remark 2.8. The imposition of the Neumann boundary conditions does not pose any particular problem in a mesh that is not aligned with Γ_N . These kinds of conditions are natural for the Stokes problem, *i.e.*, they can be enforced through a boundary integral as long as suitable quadrature rules in the cut elements are available, see [2].

Motivated by the previous remark, we henceforth assume that $\Gamma_N \cap \Gamma_T = \emptyset$, so that $\Gamma_T \subseteq \Gamma_D$, *i.e.*, we impose Dirichlet boundary conditions on the trimming curve.

3. LACK OF STABILITY OF THE NITSCHÉ METHOD

Throughout this section, we want to show with some numerical experiences that the Nitsche formulation of the Stokes problem (3), discretized with Raviart-Thomas, Nédélec, and Taylor-Hood elements, lacks stability when working on trimmed geometries. It is well-known (see [10, 40]) that the following are necessary conditions for the well-posedness of formulation (3) for both $m \in \{0, 1\}$.

(1) There exists $\bar{\gamma} > 0$ such that, for every fixed $\gamma \geq \bar{\gamma}$, there exists $M_a > 0$ such that

$$|a_h(\mathbf{w}_h, \mathbf{v}_h)| \leq M_a \|\mathbf{w}_h\|_{1,h} \|\mathbf{v}_h\|_{1,h}, \quad \forall \mathbf{w}_h, \mathbf{v}_h \in V_h. \quad (4)$$

(2) There exist $\beta_1 > 0, \beta_0 > 0$ such that

$$\inf_{q_h \in Q_h} \sup_{\mathbf{v}_h \in V_h} \frac{b_1(\mathbf{v}_h, q_h)}{\|q_h\|_{0,h} \|\mathbf{v}_h\|_{1,h}} \geq \beta_1, \quad (5)$$

$$\inf_{q_h \in Q_h} \sup_{\mathbf{v}_h \in V_h} \frac{b_0(\mathbf{v}_h, q_h)}{\|q_h\|_{0,h} \|\mathbf{v}_h\|_{1,h}} \geq \beta_0. \quad (6)$$

Remark 3.1. We observe that M_a depends (and grows dependently) on γ , which has to be taken sufficiently large, *i.e.*, $\gamma \geq \bar{\gamma}$, but at the same time as small as possible, *i.e.*, close to $\bar{\gamma}$, in order not to end up with a too-large continuity constant.

We want to show that the stability constants in the previous estimates, M_a, β_1, β_0 , can be arbitrarily negatively influenced by the relative position between the mesh and the trimming curve; hence they are not uniform with respect to the trimming operation. Note that in the following essential boundary conditions are enforced on the whole boundary, and they are weakly imposed on the parts unfitted with the mesh. Let us proceed in order.

- (1) The breakdown example for the robustness of the continuity constant M_a is the following. Let $\Omega_0 = (0, 1)^2$, $\Omega_1 = (0, 1) \times (0.75 + \varepsilon, 1)$ and $\Omega = \Omega_0 \setminus \bar{\Omega}_1$, as illustrated in Figure 1a. Note that the continuity constant of $a_h(\cdot, \cdot)$ corresponding to $\gamma = 1$ is smaller than the one related to $\gamma > 1$, *i.e.*, $M_a^\gamma > M_a^1$ for every $\gamma > 1$. Hence, in order to verify that the continuity constant also degenerates with the cut, it is sufficient to show that M_a^1 grows as ε gets smaller. M_a^1 can be estimated as the largest eigenvalue of the subsequent generalized eigenvalue problem.

Find $(\mathbf{u}_h, \lambda_h) \in V_h \setminus \{0\} \times \mathbb{R}$ such that

$$a_h(\mathbf{u}_h, \mathbf{v}_h) = \lambda_h (\mathbf{u}_h, \mathbf{v}_h)_{1,h}, \quad \forall \mathbf{v}_h \in V_h. \quad (7)$$

Assume that the mesh is uniform and let us fix the degree $k = 2$.

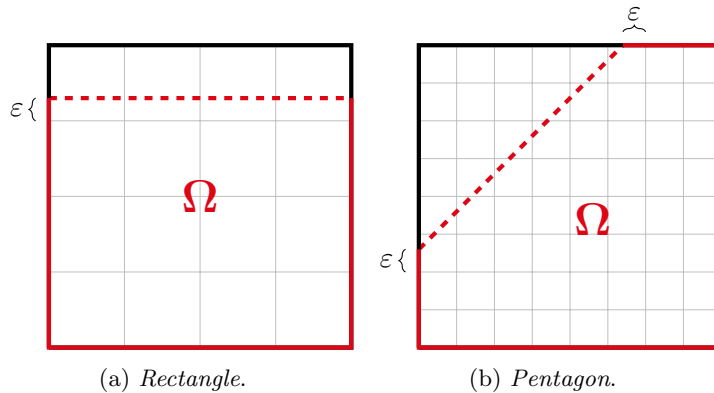


FIGURE 1. The trimmed geometries.

Then, let us compute λ_h^{\max} for different values of ε : in each configuration we refine the mesh, see Figure 2. We can clearly see how the largest eigenvalue grows unboundedly as ε goes to zero, implying that the continuity constant can be made arbitrarily large by reducing ε . As already observed in the literature in the case of the Poisson problem [14], this is due to the lack of an inverse inequality robust with respect to the trimming operation, namely,

$$\left\| \mathbf{h}^{\frac{1}{2}} D\mathbf{v}_h \mathbf{n} \right\|_{L^2(\Gamma_K)} \leq C \|D\mathbf{v}_h\|_{L^2(K \cap \Omega)},$$

with C independent of the shape and diameter of $K \cap \Omega$.

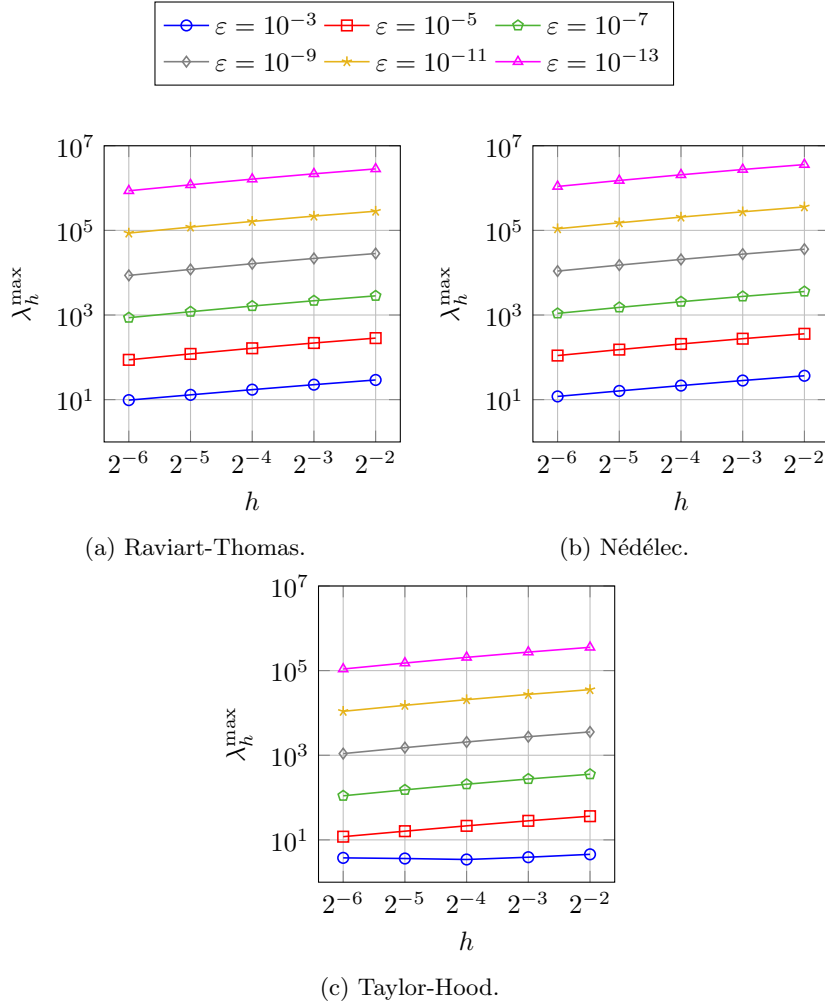
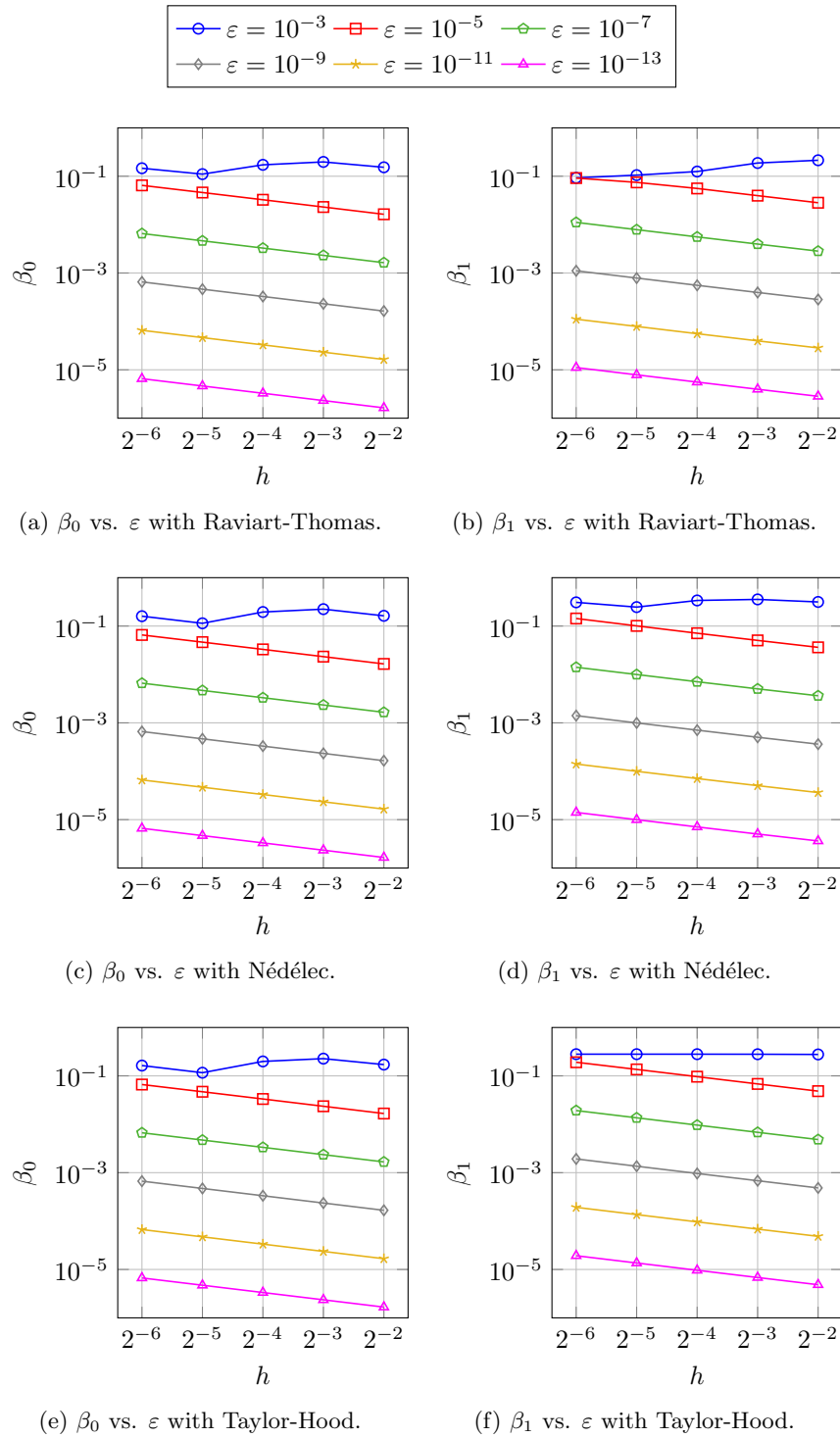


FIGURE 2. Maximum generalized eigenvalue of (7) for the trimmed *rectangle*.

- (2) Now, we consider a different setting. Let $\Omega_0 = (0, 1)^2$, Ω_1 be the triangle with vertices $(0, 0.25 + \varepsilon) - (0, 1) - (0.75 - \varepsilon, 1)$ and $\Omega = \Omega_0 \setminus \overline{\Omega_1}$, see Figure 1b. We want to study the values of β_m , $m \in \{0, 1\}$, with respect to the trimming parameter ε . The inf-sup constants are numerically evaluated as explained in [5]. In Figure 3 we plot β_m for $k = 2$ and different values of the trimming parameter ε and the mesh-size h . The numerical experiments show the dependence of β_m on ε . This negative result is due to the presence of a *spurious pressure mode* p_h^ε (technically speaking it is not spurious since, even if $\beta_m(p_h^\varepsilon) \ll 1$, it still holds $\beta_m(p_h^\varepsilon) \neq 0$) whose support is concentrated in trimmed elements with a very small overlap with the physical domain Ω .

Remark 3.2. Let us observe that in the previous numerical counterexamples, in order to validate the lack of stability of the formulation, one should have constructed a sequence of spaces depending on ε rather than changing the domain (as it is done in [14], where the lack of stability of the Nitsche formulation for the Poisson problem on trimmed domains is shown). However, both constructions lead to the same results, and we believe

FIGURE 3. Inf-sup constants for the trimmed *pentagon*.

that our choice makes the presentation more fluent. We also note that in the first counterexample, the inf-sup condition is not violated, and, similarly, the second configuration is not a counterexample for the continuity.

4. THE STABILIZED NITSCHKE FORMULATION

4.1. Stabilization procedure

We start by subdividing, for each $h > 0$, the elements of the active physical Bézier mesh \mathcal{M}_h into two disjoint collections: the one of the good elements \mathcal{M}_h^g , those with sufficient overlap with the physical domain, and the one of the bad elements \mathcal{M}_h^b , a small portion of which intersect Ω . Then, for each bad element K , we select a good neighbor K' .

Definition 4.1. Let $\theta \in (0, 1]$ be the *volume-ratio threshold* and $Q \in \widehat{\mathcal{M}}_h$. We say that Q is a *good element* if

$$\frac{|\widehat{\Omega} \cap Q|}{|Q|} \geq \theta.$$

Otherwise, Q is a *bad element*. Thanks to the regularity Assumption 2.1 on \mathbf{F} , this classification on the parametric elements naturally induces a classification on the physical elements. \mathcal{M}_h^g stands for the collection of the good physical Bézier elements and \mathcal{M}_h^b for the one of the bad physical elements. Note that $\mathcal{M}_h \setminus \mathcal{G}_h \subseteq \mathcal{M}_h^g$ and $\mathcal{M}_h^b \subseteq \mathcal{G}_h$. We denote the set of *neighbors* of K as

$$\mathcal{N}(K) := \{K' \in \mathcal{M}_h : \text{dist}(K, K') \leq Ch\} \setminus \{K\}, \quad (8)$$

where C does not depend on the mesh size nor on the trimming configuration.

The following assumption is not restrictive and is satisfied whenever the mesh is sufficiently refined, and we take C large enough in (8).

Assumption 4.2. We assume that for any $K \in \mathcal{M}_h^b$, there exists $K' \in \mathcal{N}(K) \cap \mathcal{M}_h^g$. From now on we will refer to such K' as a *good neighbor* of K .

We also define $\overline{\Omega}_{I,h} = \bigcup_{K \in \mathcal{M}_h \setminus \mathcal{G}_h} \overline{K}$, the region occupied by untrimmed elements, and $S_h := \Omega \setminus \bigcup_{K \in \mathcal{M}_h^g} \overline{K} = \text{int} \bigcup_{K \in \mathcal{M}_h^b} \overline{K} \cap \overline{\Omega}$, the region occupied by bad elements.

It is well known that formulation (3) is stable if $\Omega = \Omega_{I,h}$. In the general case $\Omega_{I,h} \subsetneq \Omega$, the goal of the stabilization is, informally speaking, to extend the stability of the discrete problem from the internal elements of the domain to the cut ones.

Remark 4.3. We observe that choosing $\theta = 1$ in Definition 4.1 corresponds to stabilizing all cut elements, in which case it holds $\mathcal{M}_h^b = \mathcal{G}_h$, $\overline{\Omega}_{I,h} = \bigcup_{K \in \mathcal{M}_h^g} \overline{K}$ and $S_h = \Omega \setminus \overline{\Omega}_{I,h}$.

Let us start by stabilizing the pressures. We define the operator $R_h^p : Q_h \rightarrow L^2(\Omega)$ locally as $R_h^p(q_h)|_K := R_K^p(q_h)$, for every $K \in \mathcal{M}_h$ and all $q_h \in Q_h$, as follows:

- if $K \in \mathcal{M}_h^g$, then

$$R_K^p(q_h) := q_h|_K,$$

- if $K \in \mathcal{M}_h^b$, then

$$R_K^p(q_h) := \mathcal{E}_{K',K} \left(\Pi_{K'}(q_h|_{K'}) \right) |_K,$$

where $\Pi_{K'} : L^2(K') \rightarrow \mathbb{Q}_k(K')$ is the local L^2 -projection and $\mathcal{E}_{K',K} : \mathbb{Q}_k(K') \rightarrow \mathbb{Q}_k(K' \cup K)$ is the canonical polynomial extension. K' is a good neighbor of K .

Proposition 4.4 (Stability property of R_h^p). *Given $\theta \in (0, 1]$, there exist $C_1, C_2 > 0$ such that, for every $K \in \mathcal{M}_h$ and $h > 0$,*

$$\begin{aligned} \left\| h^{\frac{1}{2}} R_h^p(q_h) \right\|_{L^2(\Gamma_K)} &\leq C_1 \|q_h\|_{L^2(K' \cap \Omega)}, & \forall q_h \in Q_h, \\ \|R_h^p(q_h)\|_{L^2(K \cap \Omega)} &\leq C_2 \|q_h\|_{L^2(K' \cap \Omega)}, & \forall q_h \in Q_h, \end{aligned}$$

where K' is a good neighbor if $K \in \mathcal{M}_h^b$, $K' = K$ and if $K \in \mathcal{M}_h^g$.

Proof. Let $q_h \in Q_h^\square$, $\square \in \{\text{TH}, \text{RT}, \text{N}\}$, and $K \in \mathcal{M}_h$. We first assume $K \in \mathcal{M}_h^g$ and let $Q = \mathbf{F}^{-1}(K)$, $\hat{q}_h = q_h \circ \mathbf{F}$ if $\square = \text{TH}$, $q_h = \det(D\mathbf{F})^{-1} \hat{q}_h \circ \mathbf{F}^{-1}$ if $\square \in \{\text{RT}, \text{N}\}$. Hölder's inequality, Lemma A.3, and Lemma 2.5 imply

$$\begin{aligned} \left\| h^{\frac{1}{2}} q_h \right\|_{L^2(\Gamma_K)} &= h^{\frac{1}{2}} \|q_h\|_{L^2(\Gamma_K)} \leq h^{\frac{1}{2}} |\Gamma_K|^{\frac{1}{2}} \|q_h\|_{L^\infty(\Gamma_K)} \leq h^{\frac{1}{2}} |\Gamma_K|^{\frac{1}{2}} \|q_h\|_{L^\infty(K)} \\ &\leq C_\square h^{\frac{1}{2}} |\Gamma_K|^{\frac{1}{2}} \|\hat{q}_h\|_{L^\infty(Q)} \leq C_\square h^{\frac{1}{2}} |\Gamma_K|^{\frac{1}{2}} h_K^{-\frac{d}{2}} \|\hat{q}_h\|_{L^2(Q \cap \hat{\Omega})} \leq CC_\square \bar{C}_\square \|q_h\|_{L^2(K \cap \Omega)}, \end{aligned}$$

where $C_{\text{TH}} = 1$, $C_{\text{RT}} = C_{\text{N}} = \|\det D\mathbf{F}^{-1}\|_{L^\infty(K)}$, $\bar{C}_{\text{TH}} = \|\det D\mathbf{F}^{-1}\|_{L^\infty(K \cap \Omega)}^{\frac{1}{2}}$, $\bar{C}_{\text{RT}} = \bar{C}_{\text{N}} = \|\det D\mathbf{F}\|_{L^\infty(Q \cap \hat{\Omega})}^{\frac{1}{2}}$, and C depends on k , and on θ . Now, let $K \in \mathcal{M}_h^b$ with good neighbor K' . We employ, respectively, Hölder's inequality, Lemma 2.5, and Lemma A.2, and we get

$$\begin{aligned} \left\| h^{\frac{1}{2}} R_K^p(q_h) \right\|_{L^2(\Gamma_K)} &= h^{\frac{1}{2}} \|\mathcal{E}_{K',K}(\Pi_{K'}(q_h))\|_{L^2(\Gamma_K)} \leq h^{\frac{1}{2}} |\Gamma_K|^{\frac{1}{2}} \|\mathcal{E}_{K',K}(\Pi_{K'}(q_h))\|_{L^\infty(\Gamma_K)} \\ &\leq Ch_K^{\frac{d}{2}} \|\mathcal{E}_{K',K}(\Pi_{K'}(q_h))\|_{L^\infty(K)} \leq Ch_K^{\frac{d}{2}} \|\Pi_{K'}(q_h)\|_{L^\infty(K')}. \end{aligned}$$

We can now use Lemma A.4, the boundedness of the L^2 -projection with respect to $\|\cdot\|_{L^2}$ and the local quasi-uniformity of the mesh, to obtain

$$\left\| h^{\frac{1}{2}} R_K^p(q_h) \right\|_{L^2(\Gamma_K)} \leq Ch_K^{\frac{d}{2}} h_{K'}^{-\frac{d}{2}} \|\Pi_{K'}(q_h)\|_{L^2(K')} \leq C \|q_h\|_{L^2(K')},$$

with C depending on k . By applying Hölder's inequality, moving to the parametric domain, using Lemma A.3, and moving back to the physical domain, we get

$$\begin{aligned} \left\| h^{\frac{1}{2}} R_K^p(q_h) \right\|_{L^2(\Gamma_K)} &\leq Ch_K^{\frac{d}{2}} \|q_h\|_{L^\infty(K')} \leq C_\square h_{K'}^{\frac{d}{2}} \|\hat{q}_h\|_{L^\infty(Q')} \\ &\leq CC_\square h_{K'}^{\frac{d}{2}} h_{Q'}^{-\frac{d}{2}} \|\hat{q}_h\|_{L^\infty(Q' \cap \hat{\Omega})} \leq CC_\square \bar{C}_\square \|q_h\|_{L^2(K' \cap \Omega)}, \end{aligned} \tag{9}$$

where C depends, in particular, on k and θ , and $C_\square, \bar{C}_\square$ have been defined above.

Let us move to the proof of the other inequality of the statement. If $K \in \mathcal{G}_h^g$, then there is nothing to prove. Let $K \in \mathcal{G}_h^b$ and K' its good neighbor.

$$\begin{aligned} \|R_h^p(q_h)\|_{L^2(K \cap \Omega)} &\leq |K \cap \Omega|^{\frac{1}{2}} \|R_h^p(q_h)\|_{L^\infty(K \cap \Omega)} \leq |K \cap \Omega|^{\frac{1}{2}} \|R_h^p(q_h)\|_{L^\infty(K)} \\ &\leq C |K \cap \Omega|^{\frac{1}{2}} \|\Pi_{K'}(q_h)\|_{L^\infty(K')}, \end{aligned}$$

where we have used, respectively, Hölder's inequality and Lemma A.2. Note that it is trivial to check that, for every $u \in L^2(K')$, $\|\Pi_{K'}(u)\|_{L^2(K')} \leq \|u\|_{L^2(K')}$. On the other hand, by using Lemma A.4, and the L^2 -stability

of the L^2 -projection, we have $\|\Pi_{K'}(q_h)\|_{L^\infty(K')} \leq Ch_{K'}^{-\frac{d}{2}} \|\Pi_{K'}(q_h)\|_{L^2(K')} \leq Ch_{K'}^{-\frac{d}{2}} \|q_h\|_{L^2(K')}$. Hence,

$$\|R_h^p(q_h)\|_{L^2(K \cap \Omega)} \leq C |K \cap \Omega|^{\frac{1}{2}} h_{K'}^{-\frac{d}{2}} \|q_h\|_{L^2(K')} \leq C |K \cap \Omega|^{\frac{1}{2}} |K|^{-\frac{1}{2}} \|q_h\|_{L^2(K')} \leq C \|q_h\|_{L^2(K')},$$

where in the second last passage of both lines we used the shape-regularity and quasi-local uniformity of the mesh, entailing $h_{K'}^{-\frac{d}{2}} \sim |K'|^{-\frac{1}{2}}$, $|K'|^{-\frac{1}{2}} \sim |K|^{-\frac{1}{2}}$. We observe that the constant C depends on k , since we relied on Lemma A.4. We conclude as in (9). \square

Now, let us move to the velocities and define, for $\square \in \{\text{RT}, \text{N}, \text{TH}\}$, the operator $R_h^v : V_h^\square \rightarrow \mathbf{L}^2(\Omega)$ locally as $R_h^v(\mathbf{v}_h)|_K := R_K^v(\mathbf{v}_h)$ for every $K \in \mathcal{M}_h$ and all $\mathbf{v}_h \in V_h^\square$:

- if $K \in \mathcal{M}_h^g$, then

$$R_K^v(\mathbf{v}_h) := \mathbf{v}_h|_K,$$

- if $K \in \mathcal{M}_h^b$, then

$$R_K^v(\mathbf{v}_h) := \mathcal{E}_{K',K}(\mathbf{\Pi}_{K'}(\mathbf{v}_h|_{K'}))|_K,$$

where $\mathbf{\Pi}_{K'} : \mathbf{L}^2(K') \rightarrow \mathbb{V}_k(K')$ is the L^2 -orthogonal projection onto

$$\mathbb{V}_k(K') := \begin{cases} \mathbb{S}_k(K'), & \text{if } \square = \text{RT}, \\ (\mathbb{Q}_{k+1}(K'))^d, & \text{if } \square \in \{\text{N}, \text{TH}\}, \end{cases}$$

$$\mathbb{S}_k(K') := \begin{cases} \mathbb{Q}_{k+1,k}(K') \times \mathbb{Q}_{k,k+1}(K'), & \text{if } d = 2, \\ \mathbb{Q}_{k+1,k,k}(K') \times \mathbb{Q}_{k,k+1,k}(K') \times \mathbb{Q}_{k,k,k+1}(K'), & \text{if } d = 3, \end{cases}$$

and $\mathcal{E}_{K',K} : \mathbb{V}_h(K') \rightarrow \mathbb{V}_h(K \cup K')$ is the canonical polynomial extension. Here, $K' \in \mathcal{M}_h^g$ denotes a good neighbor of K .

Proposition 4.5 (Stability property of R_h^v). *Given $\theta \in (0, 1]$, there exists $C > 0$ such that, for every $K \in \mathcal{M}_h$,*

$$\left\| h^{\frac{1}{2}} DR_h^v(\mathbf{v}_h) \mathbf{n} \right\|_{L^2(\Gamma_K)} \leq C \|D\mathbf{v}_h\|_{L^2(K' \cap \Omega)}, \quad \forall \mathbf{v}_h \in V_h,$$

where $K' \in \mathcal{M}_h^g$ is a good neighbor of K if $K \in \mathcal{M}_h^b$, $K' = K$ if $K \in \mathcal{M}_h^g$.

Proof. We refer the reader to the proof of Theorem 6.8 of [14]. The constant C will depend on \mathbf{F} accordingly to the element choice. \square

As we saw in Section 3, due to the unfitted configuration, the Nitsche formulation (3) may present some serious instabilities. Our remedy is twofold. On the one hand, we locally change the evaluation of the normal derivatives of the velocities in the weak formulation; on the other, we modify the space of the discrete pressures.

We introduce the following *stabilized pressure space*

$$\overline{Q}_h := \left\{ \varphi_h \in L^2(\Omega) : \exists q_h \in Q_h \text{ such that } \varphi_h|_{\Omega \setminus \overline{S}_h} = q_h|_{\Omega \setminus \overline{S}_h} \text{ and } \varphi_h|_{S_h} = R_h^p(q_h)|_{S_h} \right\}.$$

Remark 4.6. Let us stress that, while $\dim \overline{Q}_h \leq \dim Q_h$, in general, we have that \overline{Q}_h is not a subspace of Q_h since its elements are discontinuous functions. However, we observe that the discontinuities are located across the facets in the region of bad elements \overline{S}_h and, for $q_h \in Q_h$ and $R_h^p(q_h) \in \overline{Q}_h$, it holds

$$q_h|_{\Omega \setminus \overline{S}_h} = R_h^p(q_h)|_{\Omega \setminus \overline{S}_h}.$$

Remark 4.7. Proposition 4.4 entails that $\|\cdot\|_{0,h}$ and $\|\cdot\|_{L^2(\Omega \setminus \bar{\mathcal{S}}_h)}$ are equivalent norms on \bar{Q}_h , namely there exist $c_1, c_2 > 0$, independent on h and on the way the mesh is cut by trimming curve, but in general depending on the fixed parameter $\theta \in (0, 1]$, such that

$$c_1 \|q_h\|_{L^2(\Omega \setminus \bar{\mathcal{S}}_h)} \leq \|q_h\|_{0,h} \leq c_2 \|q_h\|_{L^2(\Omega \setminus \bar{\mathcal{S}}_h)}, \quad \forall q_h \in \bar{Q}_h.$$

Remark 4.8. Let $Q_h = \{B_{\mathbf{k}}|_{\Omega} : \mathbf{k} \in \mathbf{K}\}$ and define $\tilde{Q}_h = \{B_{\mathbf{i}}|_{\Omega} : \mathbf{i} \in \mathbf{I}\}$, where $\mathbf{I} := \{\mathbf{i} \in \mathbf{K} : \exists K \in \mathcal{M}_h^g \text{ such that } K \subset \text{supp } B_{\mathbf{i}}\}$. This time \tilde{Q}_h is a subspace of Q_h . Moreover, let us observe that \bar{Q}_h and \tilde{Q}_h are isomorphic (as normed vector spaces) when equipped with $\|\cdot\|_{L^2(\Omega \setminus \bar{\mathcal{S}}_h)}$.

We introduce the following stabilized version of formulation (3).

Find $(\mathbf{u}_h, p_h) \in V_h \times \bar{Q}_h$ such that

$$\begin{aligned} \bar{a}_h(\mathbf{u}_h, \mathbf{v}_h) + b_1(\mathbf{v}_h, p_h) &= \bar{F}_h(\mathbf{v}_h), & \forall \mathbf{v}_h \in V_h, \\ b_m(\mathbf{u}_h, q_h) &= G_m(q_h), & \forall q_h \in \bar{Q}_h, \end{aligned} \tag{10}$$

where $m \in \{0, 1\}$ and

$$\begin{aligned} \bar{a}_h(\mathbf{w}_h, \mathbf{v}_h) &:= \int_{\Omega} D\mathbf{w}_h : D\mathbf{v}_h - \int_{\Gamma_D} DR_h^v(\mathbf{w}_h) \mathbf{n} \cdot \mathbf{v}_h - \int_{\Gamma_D} \mathbf{w}_h \cdot DR_h^v(\mathbf{v}_h) \mathbf{n} \\ &\quad + \gamma \int_{\Gamma_D} \mathbf{h}^{-1} \mathbf{w}_h \cdot \mathbf{v}_h, & \mathbf{w}_h, \mathbf{v}_h \in V_h, \\ \bar{F}_h(\mathbf{v}_h) &:= \int_{\Omega} \mathbf{f} \cdot \mathbf{v}_h + \int_{\Gamma_N} \boldsymbol{\sigma} \cdot \mathbf{v}_h - \int_{\Gamma_D} \mathbf{u}_D \cdot DR_h^v(\mathbf{v}_h) \mathbf{n} + \gamma \int_{\Gamma_D} \mathbf{h}^{-1} \mathbf{u}_D \cdot \mathbf{v}_h, & \mathbf{v}_h \in V_h. \end{aligned}$$

Remark 4.9. We believe that this strategy is still consistent with the stabilization procedure of [14] since the modification does not affect the space of the velocities, but just the one of pressures, the latter being discontinuous objects from a physical point of view.

4.2. Interpolation and approximation properties of the discrete spaces

From [30], there exist $\mathbf{E} : \mathbf{H}^t(\Omega) \rightarrow \mathbf{H}^t(\mathbb{R}^d)$, $t \geq 1$, and $E : H^r(\Omega) \rightarrow H^r(\mathbb{R}^d)$, $r \geq 1$, universal (degree-independent) Sobolev-Stein extensions such that $\text{div} \circ \mathbf{E} = E \circ \text{div}$. We define, for $\square \in \{\text{RT}, \text{N}, \text{TH}\}$ and $t \geq 1$,

$$\Pi_{V_h}^{\square} : \mathbf{H}^t(\Omega) \rightarrow V_h^{\square}, \quad \mathbf{v} \mapsto \Pi_{V_{0,h}}^{\square} \left(\mathbf{E}(\mathbf{v})|_{\Omega_0} \right) \Big|_{\Omega},$$

where $\Pi_{V_{0,h}}^{\square}$ is the spline quasi-interpolant onto $V_{0,h}^{\square}$. Similarly, for the pressures, given $r \geq 1$, we introduce

$$\Pi_{Q_h}^{\square} : H^r(\Omega) \rightarrow Q_h^{\square}, \quad q \mapsto \Pi_{Q_{0,h}}^{\square} \left(E(q)|_{\Omega_0} \right) \Big|_{\Omega},$$

and further compose it with the stabilization operator for the pressures,

$$\bar{\Pi}_{Q_h}^{\square} : H^r(\Omega) \rightarrow \bar{Q}_h^{\square}, \quad q \mapsto R_h^p \left(\Pi_{Q_h}^{\square} q \right),$$

where $\Pi_{Q_{0,h}}^{\square}$ is the spline quasi-interpolant onto $Q_{0,h}^{\square}$. Let us recall that, in the Raviart-Thomas case, $\Pi_{V_{0,h}}^{\text{RT}}$ and $\Pi_{Q_{0,h}}^{\text{RT}}$ are defined so that the first diagram in (11) commutes (see [15]). Our construction implies that also the

diagram on the right commutes.

$$\begin{array}{ccc}
\mathbf{H}(\operatorname{div}; \Omega_0) & \xrightarrow{\operatorname{div}} & L^2(\Omega_0) & \quad & \mathbf{H}(\operatorname{div}; \Omega) & \xrightarrow{\operatorname{div}} & L^2(\Omega) \\
\downarrow \Pi_{V_{0,h}}^{\operatorname{RT}} & & \downarrow \Pi_{Q_{0,h}}^{\operatorname{RT}} & & \downarrow \Pi_{V_h}^{\operatorname{RT}} & & \downarrow \Pi_{Q_h}^{\operatorname{RT}} \\
V_{0,h}^{\operatorname{RT}} & \xrightarrow{\operatorname{div}} & Q_{0,h}^{\operatorname{RT}} & & V_h^{\operatorname{RT}} & \xrightarrow{\operatorname{div}} & Q_h^{\operatorname{RT}}
\end{array} \tag{11}$$

Remark 4.10. Note that the commutativity of the right-hand diagram in (11) is lost when instead of Q_h we use the stabilized space \bar{Q}_h .

Proposition 4.11 (Approximation property of R_h^v). *There exists $C > 0$ such that, for every $\mathbf{v} \in \mathbf{H}^t(\Omega)$, $t \geq 2$, and $K \in \mathcal{G}_h$,*

$$\left\| \mathbf{h}^{\frac{1}{2}} D \left(\mathbf{v} - R_h^v(\Pi_{V_h}^{\square} \mathbf{v}) \right) \mathbf{n} \right\|_{L^2(\Gamma_D)} \leq Ch^s \|\mathbf{v}\|_{H^t(\Omega)},$$

where $s := \min\{k, t-1\}$ if $\square = \operatorname{RT}$ and $s := \min\{k+1, t-1\}$ if $\square \in \{\operatorname{N}, \operatorname{TH}\}$.

Proof. It is sufficient to apply the vectorial version of Proposition 6.9 of [14] and to sum over the cut elements in \mathcal{G}_h . The constant C depends on \mathbf{F} accordingly to the element choice. \square

Lemma 4.12. *There exists $C > 0$ such that*

$$\|\Pi_{V_h} \mathbf{v}\|_{1,h} \leq C \|\mathbf{v}\|_{H^1(\Omega)}, \quad \forall \mathbf{v} \in \mathbf{H}_{0,\Gamma_D}^1(\Omega).$$

Proof. Let $\mathbf{v} \in \mathbf{H}_{0,\Gamma_D}^1(\Omega)$. Using the H^1 -stability for the quasi-interpolant in the boundary-fitted case [15], we have

$$\|\Pi_{V_h} \mathbf{v}\|_{1,h}^2 = \|D\Pi_{V_{0,h}}(\mathbf{E}(\mathbf{v}))\|_{L^2(\Omega)}^2 + \left\| \mathbf{h}^{-\frac{1}{2}} \Pi_{V_{0,h}}(\mathbf{E}(\mathbf{v})) \right\|_{L^2(\Gamma_D)}^2 \tag{12}$$

$$\leq C \|\mathbf{E}(\mathbf{v})\|_{H^1(\Omega_0)} + \sum_{K \in \mathcal{G}_h} h_K^{-1} \|\Pi_{V_{0,h}}(\mathbf{E}(\mathbf{v}))\|_{L^2(\Gamma_K)}^2. \tag{13}$$

By using $\mathbf{E}(\mathbf{v})|_{\Gamma_D} = 0$, Lemma A.1, and the optimal approximation properties of the quasi-interpolants on boundary-fitted meshes, it holds

$$\begin{aligned}
\sum_{K \in \mathcal{G}_h} h_K^{-1} \|\Pi_{V_{0,h}}(\mathbf{E}(\mathbf{v}))\|_{L^2(\Gamma_K)}^2 &= \sum_{K \in \mathcal{G}_h} h_K^{-1} \|\Pi_{V_{0,h}}(\mathbf{E}(\mathbf{v})) - \mathbf{E}(\mathbf{v})\|_{L^2(\Gamma_K)}^2 \\
&\leq C \sum_{K \in \mathcal{G}_h} h_K^{-1} \|\Pi_{V_{0,h}}(\mathbf{E}(\mathbf{v})) - \mathbf{E}(\mathbf{v})\|_{L^2(K)} \|\Pi_{V_{0,h}}(\mathbf{E}(\mathbf{v})) - \mathbf{E}(\mathbf{v})\|_{H^1(K)} \\
&\leq C \|\mathbf{E}(\mathbf{v})\|_{H^1(\Omega_0)}^2.
\end{aligned} \tag{14}$$

We conclude by combining (12) and (14), and using the boundedness of the Sobolev-Stein extension operator. \square

Theorem 4.13. *There exist $C_v, C_q > 0$ such that for every $(\mathbf{v}, q) \in \mathbf{H}^t(\Omega) \times H^r(\Omega)$, $t \geq 1$ and $r \geq 1$, it holds*

$$\left\| \mathbf{v} - \Pi_{V_h}^{\square} \mathbf{v} \right\|_{1,h} \leq C_v h^s \|\mathbf{v}\|_{H^t(\Omega)}, \quad \|q - \bar{\Pi}_{Q_h} q\|_{0,h} \leq C_q h^\ell \|q\|_{H^r(\Omega)},$$

where $s := \min\{k, t-1\}$ if $\square = \operatorname{RT}$, $s := \min\{k+1, t-1\}$ if $\square \in \{\operatorname{N}, \operatorname{TH}\}$, and $\ell := \min\{k+1, r\}$.

Proof. For the velocities, we proceed by employing the trace inequality of Lemma A.1 componentwise, the standard approximation properties of $\Pi_{V_{0,h}}$, and the boundedness of the Sobolev-Stein extension operator.

$$\begin{aligned}
\left\| \mathbf{v} - \Pi_{V_h}^\square \mathbf{v} \right\|_{1,h}^2 &\leq \left\| D \left(\mathbf{E}(\mathbf{v}) - \Pi_{V_{0,h}}^\square \mathbf{E}(\mathbf{v}) \right) \right\|_{L^2(\Omega_0)}^2 \\
&\quad + C \sum_{K \in \mathcal{G}_h} \left\| \mathbf{h}^{-1} \left(\mathbf{E}(\mathbf{v}) - \Pi_{V_{0,h}}^\square \mathbf{E}(\mathbf{v}) \right) \right\|_{L^2(K)} \left\| \mathbf{E}(\mathbf{v}) - \Pi_{V_{0,h}}^\square \mathbf{E}(\mathbf{v}) \right\|_{H^1(K)} \\
&\leq Ch^{2s} \left\| \mathbf{E}(\mathbf{v}) \right\|_{H^t(\Omega_0)}^2 \\
&\quad + C \sum_{K \in \mathcal{G}_h} \left\| \mathbf{h}^{-1} \left(\mathbf{E}(\mathbf{v}) - \Pi_{V_{0,h}}^\square \mathbf{E}(\mathbf{v}) \right) \right\|_{L^2(K)} \left\| \mathbf{E}(\mathbf{v}) - \Pi_{V_{0,h}}^\square \mathbf{E}(\mathbf{v}) \right\|_{H^1(K)} \\
&\leq Ch^{2s} \left\| \mathbf{v} \right\|_{H^t(\Omega)}^2 + \left\| \mathbf{h}^{-1} \left(\mathbf{E}(\mathbf{v}) - \Pi_{V_h}^\square \mathbf{v} \right) \right\|_{L^2(\Omega_0)} \left\| \mathbf{E}(\mathbf{v}) - \Pi_{V_h}^\square \mathbf{v} \right\|_{H^1(\Omega_0)} \\
&\leq Ch^{2s} \left\| \mathbf{v} \right\|_{H^t(\Omega)}^2,
\end{aligned}$$

where $s := \min\{k, t-1\}$ if $\square = \text{RT}$, $s := \min\{k+1, t-1\}$ if $\square \in \{\text{N}, \text{TH}\}$. For the pressure term, we have

$$\left\| q - \bar{\Pi}_{Q_h} q \right\|_{0,h}^2 = \left\| (q - \bar{\Pi}_{Q_h} q) \right\|_{L^2(\Omega)}^2 + \sum_{K \in \mathcal{G}_h} \left\| \mathbf{h}^{\frac{1}{2}} (q - \bar{\Pi}_{Q_h} q) \right\|_{L^2(\Gamma_K)}^2. \quad (15)$$

For the volumetric term we may proceed analogously to the case of the velocities. Let us focus on the boundary part of (15) and take $K \in \mathcal{M}_h^g$. We employ Lemma A.1:

$$\begin{aligned}
\left\| \mathbf{h}^{\frac{1}{2}} (E(q) - \bar{\Pi}_{Q_h} q) \right\|_{L^2(\Gamma_K)}^2 &\leq C \left\| E(q) - \Pi_{Q_{0,h}} E(q) \right\|_{L^2(K)} \left\| \mathbf{h} (E(q) - \Pi_{Q_{0,h}} E(q)) \right\|_{H^1(K)} \\
&\leq Ch^{2\ell} \left\| E(q) \right\|_{H^r(\tilde{K})},
\end{aligned}$$

where $\ell := \min\{k+1, r\}$. Now, let us suppose $K \in \mathcal{M}_h^b$, with $K' \in \mathcal{M}_h^g$ its good neighbor. Let $\varphi \in \mathbb{Q}_k(B_K)$, where B_K is the minimal bounding box enclosing K and K' , so that $R_K^p(\varphi) = \varphi$. We have

$$\begin{aligned}
\left\| \mathbf{h}^{\frac{1}{2}} (q - \bar{\Pi}_{Q_h} q) \right\|_{L^2(\Gamma_K)} &= \left\| \mathbf{h}^{\frac{1}{2}} (q - R_K^p(\Pi_{Q_h} q)) \right\|_{L^2(\Gamma_K)} \\
&\leq \underbrace{\left\| \mathbf{h}^{\frac{1}{2}} (q - \varphi) \right\|_{L^2(\Gamma_K)}}_I + \underbrace{\left\| \mathbf{h}^{\frac{1}{2}} R_K^p(\varphi - \Pi_{Q_h} q) \right\|_{L^2(\Gamma_K)}}_{II}.
\end{aligned}$$

By using Lemma A.1, we obtain

$$I \leq C \left\| E(q) - \varphi \right\|_{L^2(K)}^{\frac{1}{2}} \left\| \mathbf{h} (E(q) - \varphi) \right\|_{H^1(K)}^{\frac{1}{2}} \leq C \left\| E(q) - \varphi \right\|_{L^2(B_K)}^{\frac{1}{2}} \left\| \mathbf{h} (E(q) - \varphi) \right\|_{H^1(B_K)}^{\frac{1}{2}}.$$

On the other hand, from Proposition 4.4 and triangular inequality we have

$$\begin{aligned}
II &= \left\| \mathbf{h}^{\frac{1}{2}} R_K^p(\varphi - \Pi_{Q_h} q) \right\|_{L^2(\Gamma_K)} \leq C \left\| (\varphi - \Pi_{Q_h} q) \right\|_{L^2(K')} \\
&\leq C \left(\left\| \varphi - q \right\|_{L^2(K')} + \left\| q - \Pi_{Q_h} q \right\|_{L^2(K')} \right) \\
&\leq C \left(\left\| \varphi - E(q) \right\|_{L^2(B_K)} + \left\| E(q) - \Pi_{0,Q_h}(E(q)) \right\|_{L^2(K')} \right).
\end{aligned}$$

Let us choose φ such that the Deny-Lions Lemma (Theorem 3.4.1 of [42]) holds on B_K and use the optimal approximation properties of $\Pi_{Q_{0,h}}$. Thus

$$\left\| h^{\frac{1}{2}} (q - \bar{\Pi}_{Q_h} q) \right\|_{L^2(\Gamma_K)} \leq I + II \leq Ch^\ell \left(\|E(q)\|_{H^r(B_K)} + \|E(q)\|_{H^r(\tilde{K}')} \right), \quad (16)$$

where $\ell := \min\{k+1, r\}$ and C depends on the shape-regularity of B_K (through Theorem 3.4.1 of [42]), on \mathbf{F} , and on the shape-regularity of the parametric Bézier mesh (through the approximation properties of $\Pi_{Q_{0,h}}$). Hence, we conclude by taking the sum over the cut elements. The final constant will depend on k, d , on the constant appearing in (8), on the shape-regularity of the parametric mesh, on \mathbf{F} , and on the boundedness of the Sobolev-Stein extension. \square

5. WELL-POSEDNESS OF THE STABILIZED FORMULATION

The following result gives the necessary and sufficient conditions for the existence, uniqueness and stability of the solution of (10). Let us denote $K_m := \{\mathbf{v}_h \in V_h : b_m(\mathbf{v}_h, q_h) = 0 \quad \forall q_h \in \bar{Q}_h\}$, for $m = 0, 1$. Even if not explicitly stated in order to keep the notation lighter, the following stability constants are required to be independent of the mesh-size h and on the way \mathcal{M}_h has been cut by Γ_T .

Proposition 5.1. *Let us fix $m \in \{0, 1\}$, i.e., we choose either the symmetric or the non-symmetric version of (10).*

(i) *There exists $\bar{\gamma} > 0$ such that, for every $\gamma \geq \bar{\gamma}$, there exists $M_a > 0$ such that*

$$|\bar{a}_h(\mathbf{w}_h, \mathbf{v}_h)| \leq M_a \|\mathbf{w}_h\|_{1,h} \|\mathbf{v}_h\|_{1,h}, \quad \forall \mathbf{w}_h, \mathbf{v}_h \in V_h. \quad (17)$$

(ii) *There exist $M_{b_1} > 0, M_{b_0} > 0$ such that*

$$|b_1(\mathbf{v}_h, q_h)| \leq M_{b_1} \|\mathbf{v}_h\|_{1,h} \|q_h\|_{0,h}, \quad \forall \mathbf{v}_h \in V_h, \forall q_h \in \bar{Q}_h, \quad (18)$$

$$|b_0(\mathbf{v}_h, q_h)| \leq M_{b_0} \|\mathbf{v}_h\|_{1,h} \|q_h\|_{0,h}, \quad \forall \mathbf{v}_h \in V_h, \forall q_h \in \bar{Q}_h. \quad (19)$$

(iii) *There exist $\bar{\gamma} > 0$ and $\alpha_m > 0$ such that, for every $\gamma \geq \bar{\gamma}$, it holds*

$$\inf_{\mathbf{v}_h \in K_m} \sup_{\mathbf{w}_h \in K_1} \frac{\bar{a}_h(\mathbf{w}_h, \mathbf{v}_h)}{\|\mathbf{w}_h\|_{1,h} \|\mathbf{v}_h\|_{1,h}} \geq \alpha_m, \quad (20)$$

and, for all $\mathbf{w}_h \in K_1 \setminus \{0\}$,

$$\sup_{\mathbf{v}_h \in K_m} \bar{a}_h(\mathbf{w}_h, \mathbf{v}_h) > 0. \quad (21)$$

(iv) *There exist $\beta_1 > 0, \beta_0 > 0$ such that*

$$\inf_{q_h \in \bar{Q}_h} \sup_{\mathbf{v}_h \in V_h} \frac{b_1(\mathbf{v}_h, q_h)}{\|q_h\|_{0,h} \|\mathbf{v}_h\|_{1,h}} \geq \beta_1, \quad (22)$$

$$\inf_{q_h \in \bar{Q}_h} \sup_{\mathbf{v}_h \in V_h} \frac{b_0(\mathbf{v}_h, q_h)}{\|q_h\|_{0,h} \|\mathbf{v}_h\|_{1,h}} \geq \beta_0. \quad (23)$$

Conditions (i)–(iv) hold if and only if there exists a unique solution $(\mathbf{u}_h, q_h) \in V_h \times \bar{Q}_h$ to (10). Moreover,

$$\begin{aligned} \|\mathbf{u}_h\|_{1,h} &\leq \frac{1}{\alpha} \|\bar{F}_h\|_{-1,h} + \frac{1}{\beta_m} \left(\frac{M_a}{\alpha} + 1 \right) \|G_m\|_{-0,h}, \\ \|p_h\|_{0,h} &\leq \frac{1}{\beta_1} \left(1 + \frac{M_a}{\alpha_m} \right) \|\bar{F}_h\|_{-1,h} + \frac{M_a}{\beta_m \beta_1} \left(\frac{M_a}{\alpha_m} + 1 \right) \|G_m\|_{-0,h}, \end{aligned} \quad (24)$$

where $\|\cdot\|_{-1,h}$ and $\|\cdot\|_{-0,h}$ denote the dual norms with respect to $\|\cdot\|_{1,h}$ and $\|\cdot\|_{0,h}$, respectively.

Proof. We refer the interested reader to [10, 40]. \square

Remark 5.2. We observe that condition (21) can be replaced by $\dim K_m = \dim K_1$. If $m = 1$, then conditions (20) and (21) can be summarized in the coercivity of $\bar{a}_h(\cdot, \cdot)$ on K_1 . Moreover, if $g \equiv 0$, then we are no more bound to satisfy (23) when $m = 0$.

Lemma 5.3. *There exist $\bar{\gamma} > 0$ and $\alpha > 0$ such that, for every $\gamma \geq \bar{\gamma}$, it holds*

$$\alpha \|\mathbf{v}_h\|_{1,h}^2 \leq \bar{a}_h(\mathbf{v}_h, \mathbf{v}_h), \quad \forall \mathbf{v}_h \in V_h,$$

and, for every $\gamma \geq \bar{\gamma}$, there exists $M_a > 0$ such that

$$|\bar{a}_h(\mathbf{w}_h, \mathbf{v}_h)| \leq M_a \|\mathbf{w}_h\|_{1,h} \|\mathbf{v}_h\|_{1,h}, \quad \forall \mathbf{w}_h, \mathbf{v}_h \in V_h.$$

Proof. This proof is based on Proposition 4.5 and follows the same lines of Theorem 5.3 of [14]. \square

During the review process of the manuscript to which this chapter refers (see [41]), we encountered an error in the proof of the conditions (22), (23). Due to the lack of time, we are compelled to require them in the form of the following assumption. The search for suitable techniques to derive such properties will be the subject of a future study.

Assumption 5.4. Given $\theta \in (0, 1]$, there exist $\beta_0 > 0$ and $\beta_1 > 0$ such that

$$\inf_{q_h \in \bar{Q}_h} \sup_{\mathbf{v}_h \in V_h} \frac{b_1(\mathbf{v}_h, q_h)}{\|q_h\|_{0,h} \|\mathbf{v}_h\|_{1,h}} \geq \beta_1, \quad \inf_{q_h \in \bar{Q}_h} \sup_{\mathbf{v}_h \in V_h} \frac{b_0(\mathbf{v}_h, q_h)}{\|q_h\|_{0,h} \|\mathbf{v}_h\|_{1,h}} \geq \beta_0.$$

Section ?? includes numerical experiments testing and confirming the validity of Assumption 5.4.

Theorem 5.5. *Let us require that Assumption 5.4 holds. For $m \in \{0, 1\}$, given $\theta \in (0, 1]$, there exists a unique solution $(\mathbf{u}_h, p_h) \in V_h^\square \times \bar{Q}_h$ of (10) satisfying the stability estimates (24).*

Proof. It suffices to verify the hypotheses of Proposition 5.1. Conditions (17), (20), (21) are implied by Lemma 5.3. The continuity bounds (18), (19) readily follow from the definitions of $\|\cdot\|_{1,h}$ and $\|\cdot\|_{0,h}$. Finally, conditions (18), (19) hold because required by Assumption 5.4. \square

6. *A priori* ERROR ESTIMATES

The goal of this section is to demonstrate that the errors, for both the velocity and pressure fields, achieve optimal *a priori* convergence rates in the topologies induced by the norms $\|\cdot\|_{1,h}$ and $\|\cdot\|_{0,h}$, respectively.

Lemma 6.1. *Let us require that Assumption 5.4 holds. Let $(\mathbf{u}, p) \in \mathbf{H}^{\frac{3}{2}+\varepsilon}(\Omega) \times H^1(\Omega)$, $\varepsilon > 0$, and $(\mathbf{u}_h, p_h) \in V_h \times \bar{Q}_h$ be the solutions of (2) and (10) with $m \in \{0, 1\}$. Then, for every $(\mathbf{u}_I, p_I) \in V_h \times \bar{Q}_h$ the following estimates hold.*

$$\begin{aligned} \|\mathbf{u}_h - \mathbf{u}_I\|_{1,h} &\leq \frac{1}{\alpha} \left(M_a \|\mathbf{u} - \mathbf{u}_I\|_{1,h} + \left\| \mathbf{h}^{\frac{1}{2}} D(\mathbf{u} - R_h^v(\mathbf{u}_I)) \mathbf{n} \right\|_{L^2(\Gamma_D)} + M_{b_1} \|p - p_I\|_{0,h} \right) \\ &\quad + \frac{1}{\beta_m} \left(1 + \frac{M_a}{\alpha} \right) M_{b_m} \|\mathbf{u} - \mathbf{u}_I\|_{1,h}, \\ \|p_h - p_I\|_{0,h} &\leq \frac{1}{\beta_1} \left(1 + \frac{M_a}{\alpha} \right) \left(M_a \|\mathbf{u} - \mathbf{u}_I\|_{1,h} + \left\| \mathbf{h}^{\frac{1}{2}} D(\mathbf{u} - R_h^v(\mathbf{u}_I)) \mathbf{n} \right\|_{L^2(\Gamma_D)} \right. \\ &\quad \left. + M_{b_1} \|p - p_I\|_{0,h} \right) + \frac{M_a}{\beta_m \beta_1} \left(1 + \frac{M_a}{\alpha} \right) M_{b_m} \|\mathbf{u} - \mathbf{u}_I\|_{1,h}. \end{aligned}$$

Proof. Let $m \in \{0, 1\}$ and $(\mathbf{u}_I, p_I) \in V_h \times \overline{Q}_h$ be arbitrary. By linearity $(\mathbf{u}_h - \mathbf{u}_I, p_h - p_I) \in V_h \times \overline{Q}_h$ satisfies the saddle point problem

$$\begin{aligned} \bar{a}_h(\mathbf{u}_h - \mathbf{u}_I, \mathbf{v}_h) + b_1(\mathbf{v}_h, p_h - p_I) &= F_I(\mathbf{v}_h), & \forall \mathbf{v}_h \in V_h, \\ b_m(\mathbf{u}_h - \mathbf{u}_I, q_h) &= G_{I,m}(q_h), & \forall q_h \in \overline{Q}_h, \end{aligned} \quad (25)$$

where

$$\begin{aligned} F_I(\mathbf{v}_h) &:= \int_{\Omega} (D(\mathbf{u} - \mathbf{u}_I) : D\mathbf{v}_h - \int_{\Gamma_D} D(\mathbf{u} - R_h^v(\mathbf{u}_I)) \mathbf{n} \cdot \mathbf{v}_h + b_1(\mathbf{v}_h, p - p_I) \\ &\quad - \int_{\Omega} (\mathbf{u} - \mathbf{u}_I) \cdot DR_h^v(\mathbf{v}_h) \mathbf{n} + \gamma \int_{\Gamma_D} h^{-1} (\mathbf{u} - \mathbf{u}_I) \cdot \mathbf{v}_h, & \mathbf{v}_h \in V_h, \\ G_{I,m}(q_h) &:= b_m(\mathbf{u} - \mathbf{u}_I, q_h), & q_h \in \overline{Q}_h. \end{aligned}$$

For the sake of completeness, let us show the first line of (25). Note that the second line follows immediately. Recall from (2) and (3) that $F(\mathbf{v}_h) = \int_{\Omega} D\mathbf{u} : D\mathbf{v}_h - \int_{\Gamma_D} D\mathbf{u} \mathbf{n} \cdot \mathbf{v}_h + b_1(\mathbf{v}_h, p)$ and $\mathbf{u}|_{\Gamma_D} = \mathbf{u}_D$. Hence

$$\begin{aligned} \bar{a}_h(\mathbf{u}_h - \mathbf{u}_I, \mathbf{v}_h) + b_1(\mathbf{v}_h, p_h - p_I) &= \bar{F}_h(\mathbf{v}_h) - \bar{a}_h(\mathbf{u}_I, \mathbf{v}_h) - b_1(\mathbf{v}_h, p_I) \\ &= F(\mathbf{v}_h) - \int_{\Omega} \mathbf{u}_D \cdot DR_h^v(\mathbf{v}_h) \mathbf{n} + \gamma \int_{\Gamma_D} h^{-1} \mathbf{u}_D \cdot \mathbf{v}_h - \int_{\Omega} D\mathbf{u}_I : D\mathbf{v}_h \\ &\quad + \int_{\Gamma_D} DR_h^v(\mathbf{u}_I) \mathbf{n} \cdot \mathbf{v}_h + \int_{\Gamma_D} \mathbf{u}_I \cdot DR_h^v(\mathbf{v}_h) \mathbf{n} - \gamma \int_{\Gamma_D} h^{-1} \mathbf{u}_I \cdot \mathbf{v}_h - b_1(\mathbf{v}_h, p_I) \\ &= \int_{\Omega} D(\mathbf{u} - \mathbf{u}_I) : D\mathbf{v}_h - \int_{\Gamma_D} D(\mathbf{u} - R_h^v(\mathbf{u}_I)) \mathbf{n} \cdot \mathbf{v}_h + b_1(\mathbf{v}_h, p - p_I) \\ &\quad - \int_{\Gamma_D} (\mathbf{u} - \mathbf{u}_I) \cdot DR_h^v(\mathbf{v}_h) \mathbf{n} + \gamma \int_{\Gamma_D} h^{-1} (\mathbf{u} - \mathbf{u}_I) \cdot \mathbf{v}_h. \end{aligned}$$

Using the stability estimates (24), respectively for $m = 0, 1$, we get

$$\begin{aligned} \|\mathbf{u}_h - \mathbf{u}_I\|_{1,h} &\leq \frac{1}{\alpha} \|F_I\|_{-1,h} + \frac{1}{\beta_m} \left(1 + \frac{M_a}{\alpha}\right) \|G_{I,m}\|_{-0,h}, \\ \|p_h - p_I\|_{0,h} &\leq \frac{1}{\beta_1} \left(1 + \frac{M_a}{\alpha}\right) \|F_I\|_{-1,h} + \frac{M_a}{\beta_m \beta_1} \left(1 + \frac{M_a}{\alpha}\right) \|G_{I,m}\|_{-0,h}. \end{aligned}$$

We conclude since, by definition of dual norm, we have

$$\begin{aligned} \|F_I\|_{-1,h} &\leq M_a \|\mathbf{u} - \mathbf{u}_I\|_{1,h} + \left\| h^{\frac{1}{2}} D(\mathbf{u} - R_h^v(\mathbf{u}_I)) \mathbf{n} \right\|_{L^2(\Gamma_D)} + M_{b_1} \|p - p_I\|_{0,h}, \\ \|G_{I,m}\|_{-0,h} &\leq M_{b_m} \|\mathbf{u} - \mathbf{u}_I\|_{1,h}. \end{aligned}$$

□

Theorem 6.2. *Let us require that Assumption 5.4 holds. Let $(\mathbf{u}, p) \in \mathbf{H}^t(\Omega) \times H^r(\Omega)$, $t \geq 2$ and $r \geq 1$, be the solution to problem (2). Then, the discrete solution $(\mathbf{u}_h, p_h) \in V_h^{\square} \times \overline{Q}_h$ of the stabilized problem (10) satisfies*

$$\|\mathbf{u} - \mathbf{u}_h\|_{1,h} + \|p - p_h\|_{0,h} \leq C_m h^{\min\{s, \ell\}} \left(\|\mathbf{u}\|_{H^t(\Omega)} + \|p\|_{H^r(\Omega)} \right),$$

where $s := \min\{k, t - 1\}$ if $\square = \text{RT}$, $s := \min\{k + 1, t - 1\}$ if $\square = \text{N}$, and $\ell := \min\{k + 1, r\}$, and $C_m > 0$ depends on the choice $m \in \{0, 1\}$ through the constants appearing in Lemma 6.1.

Proof. Given $(\mathbf{u}_I, p_I) \in V_h^\square \times \overline{Q}_h$, we proceed by triangular inequality:

$$\|\mathbf{u} - \mathbf{u}_h\|_{1,h} \leq \|\mathbf{u} - \mathbf{u}_I\|_{1,h} + \|\mathbf{u}_h - \mathbf{u}_I\|_{1,h}, \quad (26)$$

$$\|p - p_h\|_{0,h} \leq \|p - p_I\|_{0,h} + \|p_h - p_I\|_{0,h}. \quad (27)$$

Using Lemma 6.1, we obtain

$$\begin{aligned} \|\mathbf{u} - \mathbf{u}_h\|_{1,h} &\leq \|\mathbf{u} - \mathbf{u}_I\|_{1,h} + \frac{1}{\alpha} \left(M_a \|\mathbf{u} - \mathbf{u}_I\|_{1,h} + \left\| \mathbf{h}^{\frac{1}{2}} D(\mathbf{u} - R_h^v(\mathbf{u}_I)) \mathbf{n} \right\|_{L^2(\Gamma_D)} \right. \\ &\quad \left. + M_{b_1} \|p - p_I\|_{0,h} \right) + \frac{1}{\beta_m} \left(1 + \frac{M_a}{\alpha} \right) M_{b_m} \|\mathbf{u} - \mathbf{u}_I\|_{1,h}, \\ \|p - p_h\|_{0,h} &\leq \|p - p_I\|_{0,h} + \frac{1}{\beta_1} \left(1 + \frac{M_a}{\alpha} \right) \left(M_a \|\mathbf{u} - \mathbf{u}_I\|_{1,h} + \left\| \mathbf{h}^{\frac{1}{2}} D(\mathbf{u} - R_h^v(\mathbf{u}_I)) \mathbf{n} \right\|_{L^2(\Gamma_D)} \right. \\ &\quad \left. + M_{b_1} \|p - p_I\|_{0,h} \right) + \frac{M_a}{\beta_m \beta_1} \left(1 + \frac{M_a}{\alpha} \right) M_{b_m} \|\mathbf{u} - \mathbf{u}_I\|_{1,h}. \end{aligned}$$

Let us choose $\mathbf{u}_I := \Pi_{V_h^\square} \mathbf{u}$ and $p_I := \overline{\Pi}_{Q_h} p$ so that, by Proposition 4.11 and Theorem 4.13, we obtain

$$\begin{aligned} \|\mathbf{u} - \mathbf{u}_h\|_{1,h} &\leq C_v h^s \|\mathbf{u}\|_{H^t(\Omega)} + \frac{1}{\alpha} \max\{M_a, 1, M_{b_1}\} C h^{\min\{s, \ell\}} \left(\|\mathbf{u}\|_{H^t(\Omega)} + \|p\|_{H^r(\Omega)} \right) \\ &\quad + \frac{1}{\beta_m} \left(1 + \frac{M_a}{\alpha} \right) M_{b_m} C_v h^s \|\mathbf{u}\|_{H^t(\Omega)}, \\ \|p - p_h\|_{0,h} &\leq C_q h^\ell \|p\|_{H^r(\Omega)} \\ &\quad + \frac{1}{\beta_1} \left(1 + \frac{M_a}{\alpha} \right) \max\{M_a, 1, M_{b_1}\} C h^{\min\{s, \ell\}} \left(\|\mathbf{u}\|_{H^t(\Omega)} + \|p\|_{H^r(\Omega)} \right) \\ &\quad + \frac{M_a}{\beta_m \beta_1} \left(1 + \frac{M_a}{\alpha} \right) M_{b_m} C_v h^s \|\mathbf{u}\|_{H^t(\Omega)}. \end{aligned}$$

□

7. NUMERICAL EXAMPLES

The main goal of the following numerical experiments is to validate the convergence results of the Theorem 6.2 and to validate the inf-sup condition that we have not been able to prove theoretically.

To prevent the conditioning number of the linear system from being excessively corrupted by the presence of basis functions whose support barely intersects the physical domain, a left-right Jacobi preconditioner is employed. This approach helps for improving the conditioning, but, as previously discussed in [14, 21], it does not completely solve its dependence on the trimming configuration: the interested reader is referred to [20] for a more sophisticated approach.

7.1. Pentagon

Let us consider as computational domain the pentagon $\Omega = \Omega_0 \setminus \overline{\Omega}_1$, where $\Omega_0 = \widehat{\Omega}_0$ and Ω_1 is the triangle of vertices $(0, 0.25 + \varepsilon) - (0, 1) - (0.75 - \varepsilon, 1)$ as illustrated in Figure 1b. Here $\varepsilon = 10^{-13}$. The following functions are chosen as manufactured solutions for the velocity and pressure fields:

$$\mathbf{u} = \left(xy^3, x^4 - \frac{y^4}{4} \right), \quad p = p_{\text{fun}} - \frac{1}{|\Omega|} \int_{\Omega} p_{\text{fun}}, \quad \text{where } p_{\text{fun}} = x^3 \cos(x) + y^2 \sin(x).$$

Dirichlet boundary conditions are weakly enforced on the boundary sides unfitted with the mesh, while on the rest, they are imposed in the strong sense (we recall from Remark 2.7 that, for the Raviart-Thomas and Nédélec element, we need to impose the tangential components in a weak sense). We compare, for different isogeometric elements, the well-posedness and accuracy of the non-symmetric, *i.e.*, with $m = 0$, non-stabilized and stabilized formulations, (3) and (10) respectively, for $k = 2$ and $\gamma = 20(k + 1)^2$ (the dependency of the penalty parameter on the degree is coherent with [22]). The threshold parameter θ is set equal to 1, *i.e.*, all cut elements are stabilized.

In Table 1 we see the values of the inf-sup constants β_0 , β_1 , computed as in [5], in the non-stabilized and stabilized cases (subscripts *ns* and *s* respectively) for the different choices of the isogeometric element (superscripts RT, N and TH). In the stabilized case, we observe that the inf-sup constants lost their dependence on how the mesh is trimmed. In Figure 4 the accuracy of the non-stabilized and stabilized formulations are compared. We observe a clear improvement in the pressure error between the non-stabilized and the stabilized case.

h	2^{-1}	2^{-2}	2^{-3}	2^{-4}	2^{-5}	2^{-6}
$\beta_{0,ns}^{\text{RT}}$	0.2437	1.6450e-07	2.3014e-07	3.2638e-07	4.6166e-07	6.5221e-07
$\beta_{1,ns}^{\text{RT}}$	0.2699	2.8358e-07	3.9759e-07	5.5849e-07	7.8738e-07	1.1108e-06
$\beta_{0,s}^{\text{RT}}$	0.4103	0.1740	0.2032	0.1850	0.1588	0.1635
$\beta_{1,s}^{\text{RT}}$	0.3923	0.2088	0.2397	0.2440	0.2441	0.2442
$\beta_{0,ns}^{\text{N}}$	0.2714	1.6541e-07	2.3212e-07	3.2900e-07	4.6583e-07	6.5811e-07
$\beta_{1,ns}^{\text{N}}$	0.3178	3.6259e-07	5.0472e-07	7.0780e-07	9.9752e-07	1.4077e-06
$\beta_{0,s}^{\text{N}}$	0.4142	0.2430	0.2902	0.2803	0.2809	0.2676
$\beta_{1,s}^{\text{N}}$	0.4118	0.2564	0.2979	0.3089	0.3096	0.3096
$\beta_{0,ns}^{\text{TH}}$	0.2672	1.6728e-07	2.3504e-07	3.3295e-07	4.7052e-07	4.7052e-07
$\beta_{1,ns}^{\text{TH}}$	0.2768	4.8359e-07	6.8222e-07	9.6265e-07	1.3581e-06	1.9189e-06
$\beta_{0,s}^{\text{TH}}$	0.3374	0.2836	0.2853	0.2853	0.2853	0.2853
$\beta_{1,s}^{\text{TH}}$	0.2994	0.2755	0.2789	0.2802	0.2807	0.2809

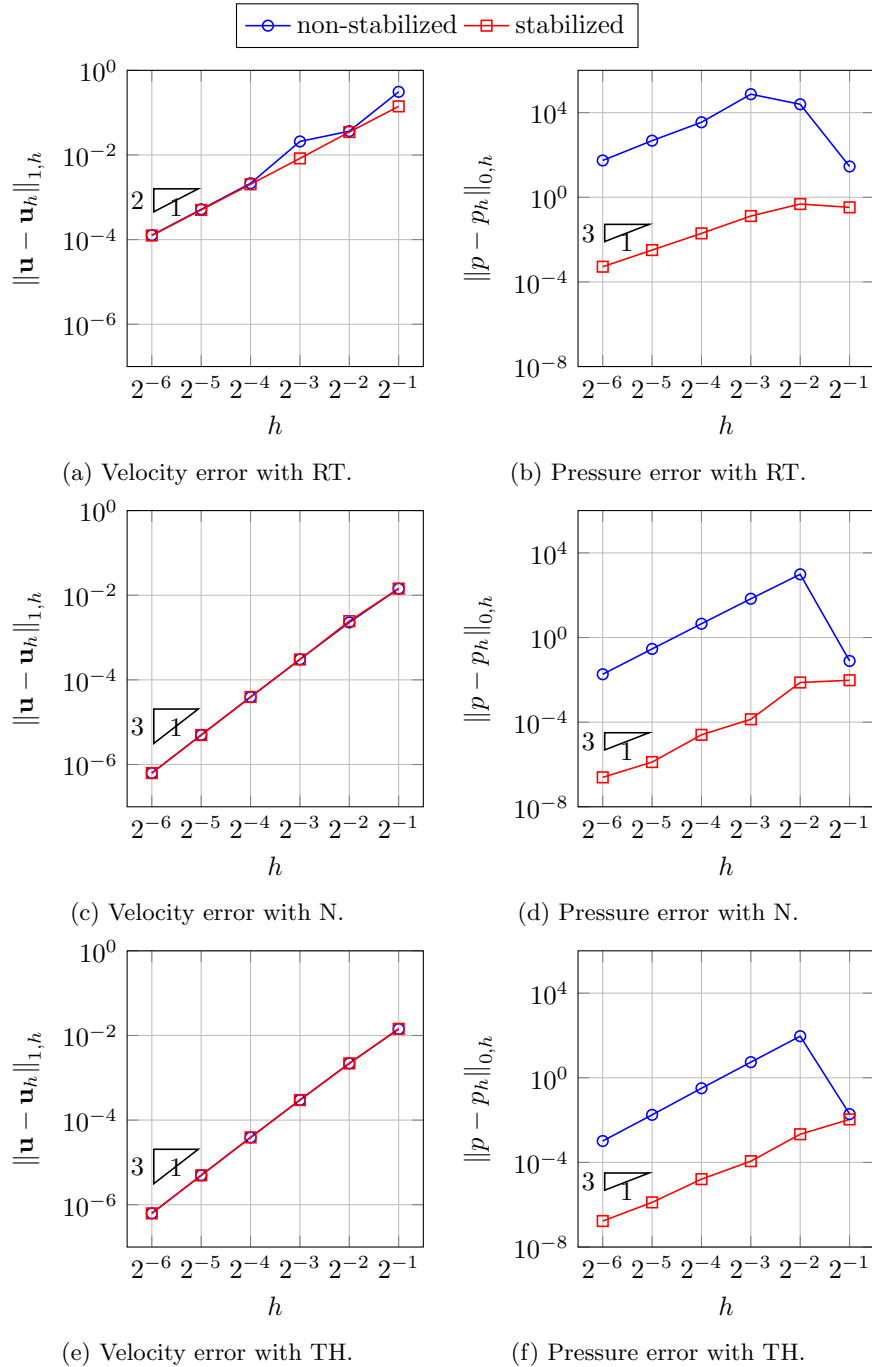
TABLE 1. Inf-sup constant for the *pentagon*: stabilized vs non-stabilized formulations with $k = 2$.

7.2. Mapped pentagon

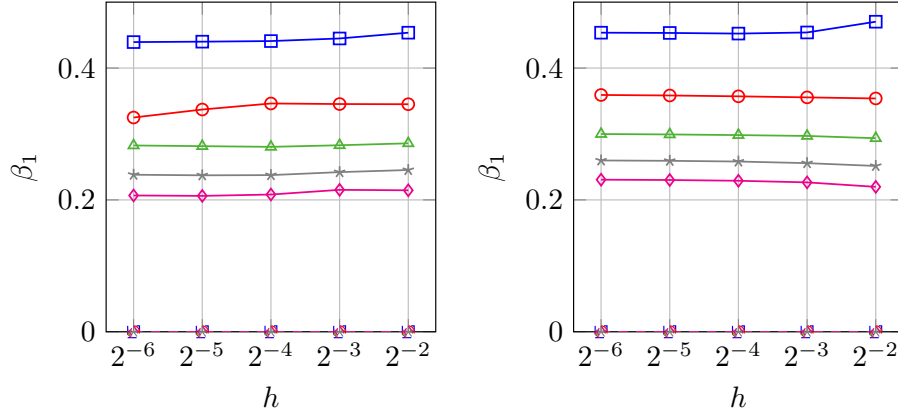
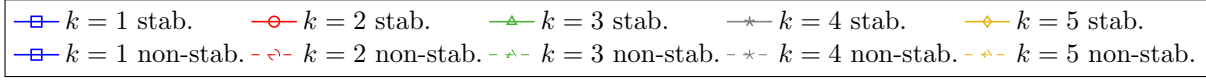
Let us perform an experiment similar to the previous one, this time with a non-linear isogeometric mapping \mathbf{F} . We consider $\Omega = \Omega_0 \setminus \overline{\Omega}_1$, where $\Omega_0 = \mathbf{F}((0,1)^2)$ is the quarter of annulus parametrized by a biquadratic NURBS \mathbf{F} , and $\Omega_1 = \mathbf{F}(T)$, with T the triangle with vertices $(0, 0.25 + \varepsilon)$, $(0, 1)$, $(0.75 - \varepsilon, 1)$, see Figure 6a. We compare the inf-sup stability of the non-stabilized and the stabilized formulations (3) and (10) respectively, for different degrees and isogeometric elements, $\theta = 1$ (we stabilize at all cut elements), and $\varepsilon = 10^{-13}$. Dirichlet boundary conditions are imposed on the whole boundary, weakly on the unfitted parts. From Figure 5 we observe that the inf-sup constants of the stabilized formulation behave much better than the ones of the non-stabilized formulation. The order of magnitude of the inf-sup constants in the non-stabilized case are of the same order of the ones in Table 1.

7.3. Rotating square

We embed $\Omega = (0.19, 0.71) \times (0.19, 0.71)$ into $\Omega_0 = (0, 1)^2$, the latter subdivided with a Cartesian grid of 8 elements per direction, and rotate Ω around its barycenter for different angles α , as illustrated in Figure 6???. We choose a threshold parameter $\theta = 0.75$, and, for each angle $\alpha \in \{i \frac{\pi}{200} : i = 0, \dots, 100\}$, we compute the inf-sup constants β_0 and β_1 in the stabilized and non-stabilized cases. For every configuration we compute

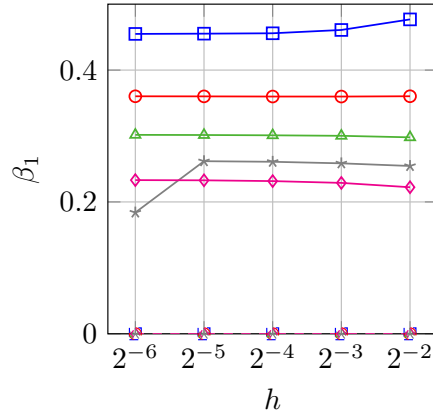
FIGURE 4. Convergence errors for the *pentagon* with $k = 2$.

$\eta := \min_{K \in \mathcal{M}_h} |K \cap \Omega|$ and in Figure 7 we plot the inf-sup constants with respect to η for the Raviart-Thomas, the



(a) Raviart-Thomas.

(b) Nédélec.



(c) Taylor-Hood.

FIGURE 5. Inf-sup constant for the *mapped pentagon* .

Nédélec, and the Taylor-Hood elements of degree $k = 2$. In most configurations, we can observe that the constants corresponding to the stabilized formulation perform better than those of the non-stabilized formulation, specially for small values of η .

Furthermore, we notice a greater efficiency, *i.e.*, a greater difference between stabilized and non-stabilized cases, when using the Taylor-Hood element. The configurations corresponding to a smaller η do not necessarily give rise to a worse inf-sup constant. Although stabilization does not always seem to “beat” the non-stabilized method, we observe that the configurations in which the non-stabilized inf-sup constant is larger than the stabilized one are, in general, the ones with bigger values of η , which are not the most critical ones.

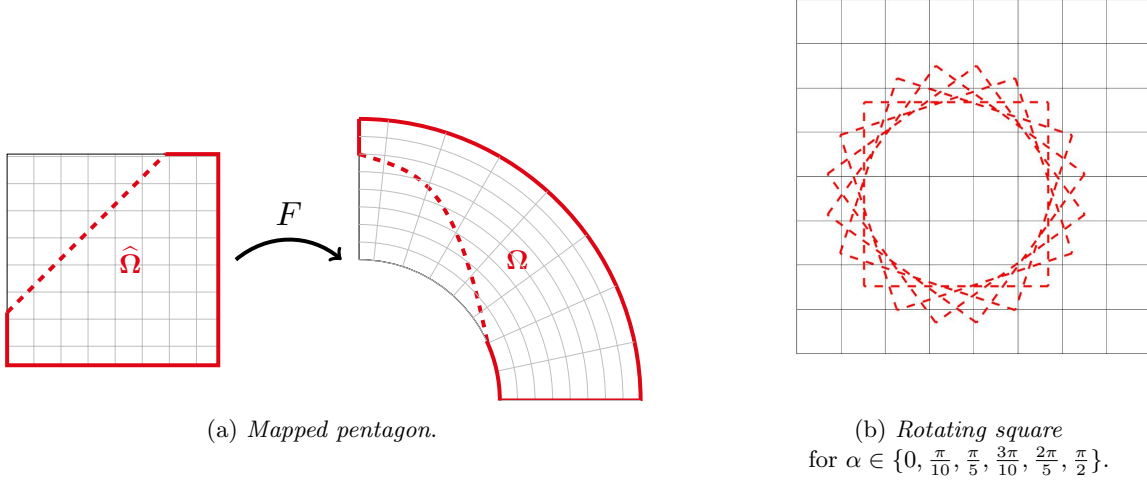


FIGURE 6. Trimmed domains.

7.4. Square with circular trimming

Let us set up another numerical experience where the physical domain is $\Omega = \Omega_0 \setminus \bar{\Omega}_1$ with $\Omega_0 = (0, 2) \times (0, 2)$ and $\Omega_1 = B(0, r)$, $r = 0.52$, as depicted in Figure 8a. We take as reference solution fields

$$\mathbf{u} = \left(2y^3 \sin(x), x^3 \sin(x) - \frac{y^4 \cos(x)}{2} - 3x^2 \cos(x) \right), \quad p = \frac{x^3 y^2}{2} + \frac{y^3}{2},$$

where \mathbf{u} is a solenoidal vector field. We impose Neumann boundary conditions on the straight trimmed sides $\{(0, y) : 0 \leq y \leq 2\}$, $\{(x, 0) : 0 \leq x \leq 2\}$ and on the rest of the boundary we impose Dirichlet boundary conditions, enforced in a weak sense on $\{(r \cos \theta, r \sin \theta) : 0 \leq \theta \leq \frac{\pi}{2}\}$. We solve using the non-symmetric stabilized formulation (10), discretized with the Raviart-Thomas element, with different degrees $k = 1, 2, 3, 4, 5$, penalty parameter $\gamma = 10(k+2)^2$, and threshold parameter $\theta = 1$. The convergence results, validating the error estimates of Theorem 6.2, are shown in Figure 9, while the divergence of the discrete velocity field \mathbf{u}_h , for $k = 3$ and $h = 2^{-4}$, has been plotted in Figure 8b. As already observed in Remark 4.10, our numerical scheme does not preserve exactly the incompressibility constraint since $\text{div } V_h^{\text{RT}} \notin \bar{Q}_h$. From Figure 8b, we can observe that the divergence of the numerical solution for the velocity is polluted in the vicinity of the trimmed boundary.

7.5. Stokes flow around a cylinder

We consider a classic benchmark example in computational fluid dynamics, *i.e.*, the so-called two-dimensional *flow around a cylinder*, proposed by [6] and already seen in the context of immersogeometric methods in [31]. The incompressible flow of a fluid around a cylinder placed in a channel is studied. The physical domain is $\Omega = \Omega_0 \setminus \bar{\Omega}_1$, where $\Omega_0 = (0, L) \times (0, H)$ and $\Omega_1 = B(x_0, R)$ with $L = 2.2$, $H = 0.41$, $x_0 = (0.2, 0.2)$ and $R = 0.05$. Let us observe that Ω_1 is not symmetric with respect to Ω_0 . As Dirichlet boundary condition on the inflow boundary $\{(0, y) : 0 \leq y \leq H\}$ a parabolic horizontal profile is prescribed:

$$\mathbf{u}(0, y) = \begin{pmatrix} 4U_m y (H - y) / H^2 \\ 0 \end{pmatrix},$$

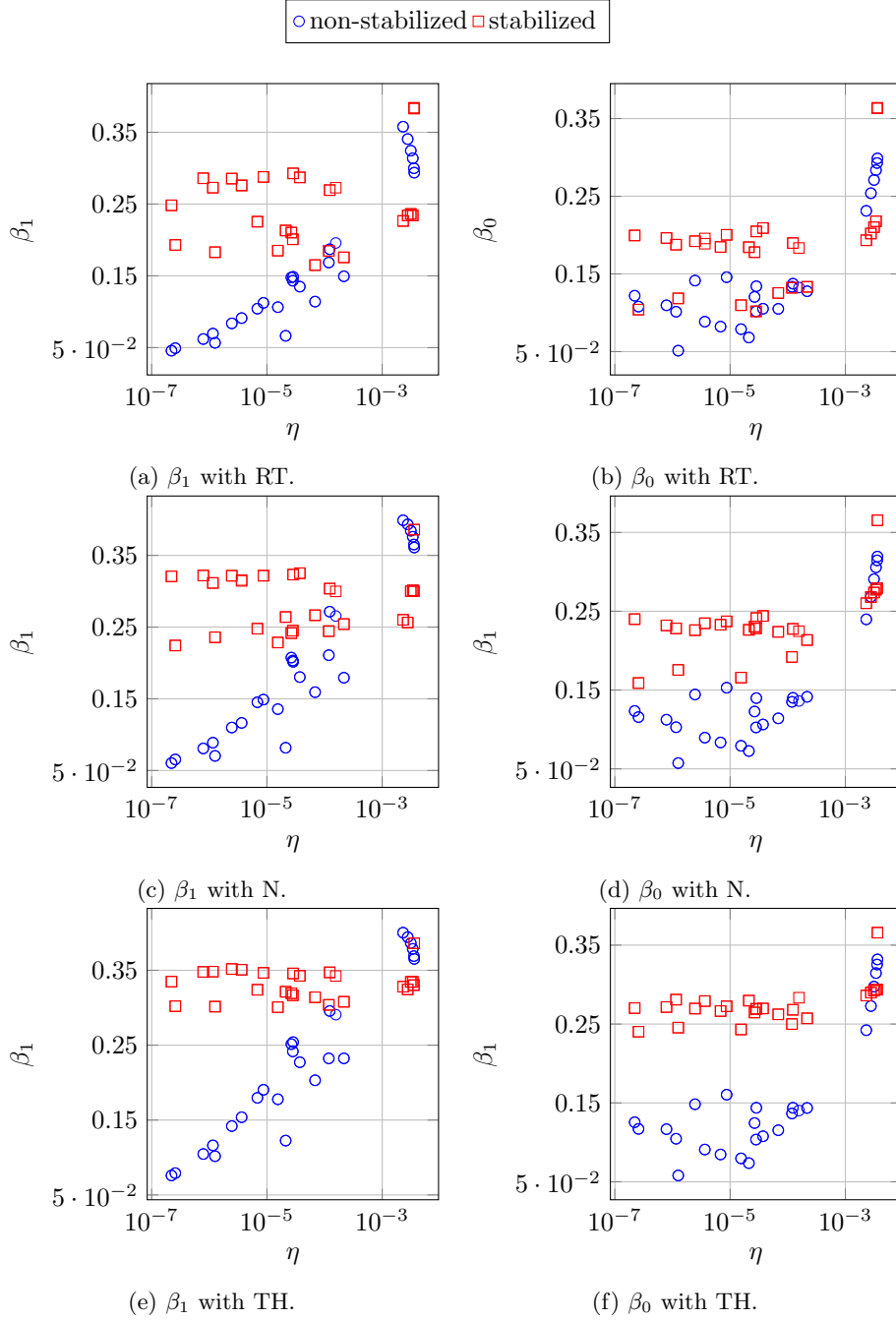


FIGURE 7. Inf-sup constants vs. the measure of the “smallest cut element”.

where $U_m = 0.3$ is the maximum magnitude of the velocity field. Stress free boundary conditions, *i.e.*, $\mathbf{u}_N = \mathbf{0}$, are imposed on the outflow boundary $\{(L, y) : 0 \leq y \leq H\}$, while no slip boundary conditions are imposed on the rest of the boundary. No external forces act on the fluid flow, *i.e.*, $\mathbf{f} = \mathbf{0}$.

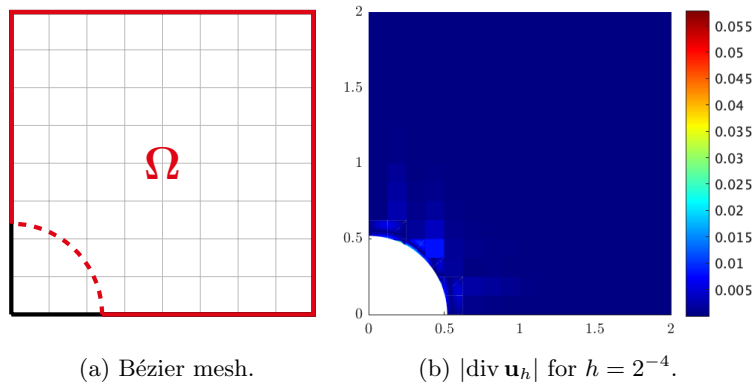
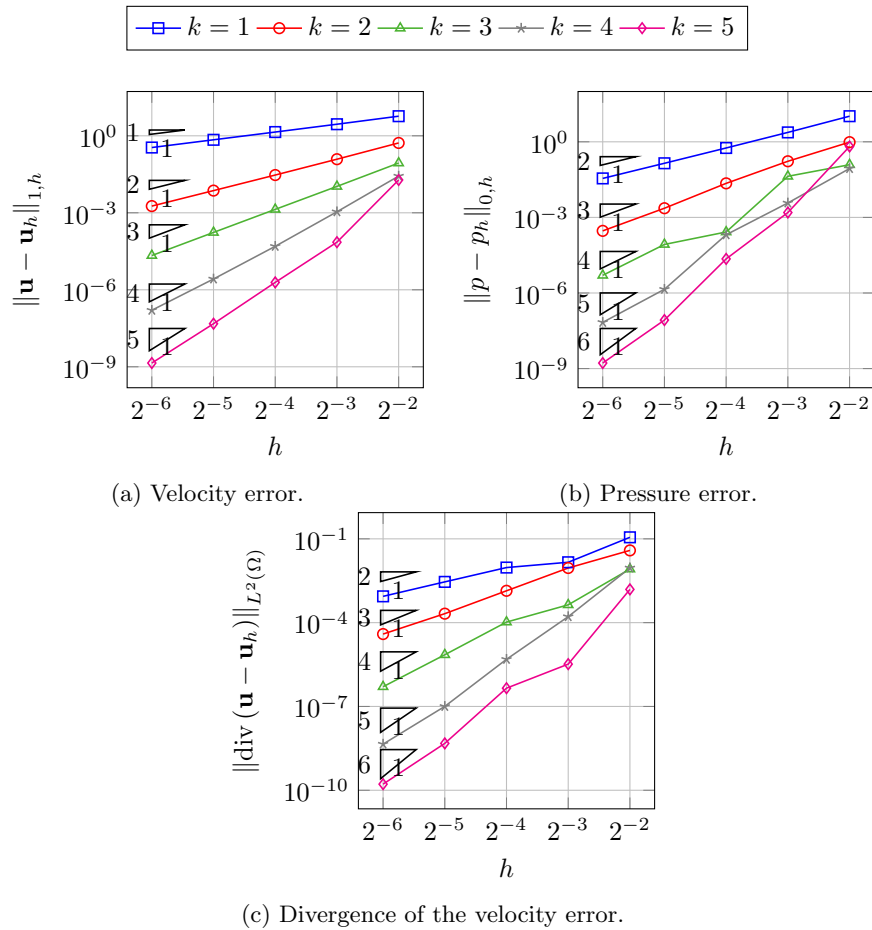


FIGURE 8. Square with circular trimming.

FIGURE 9. Convergence errors for the *Square with circular trimming* with the Raviart-Thomas element.

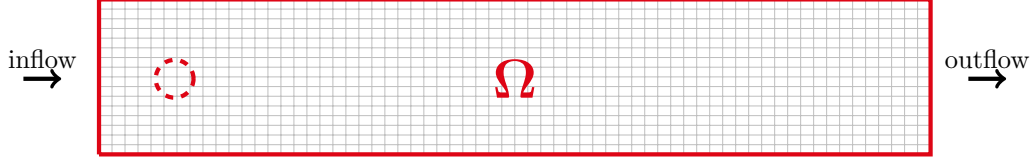
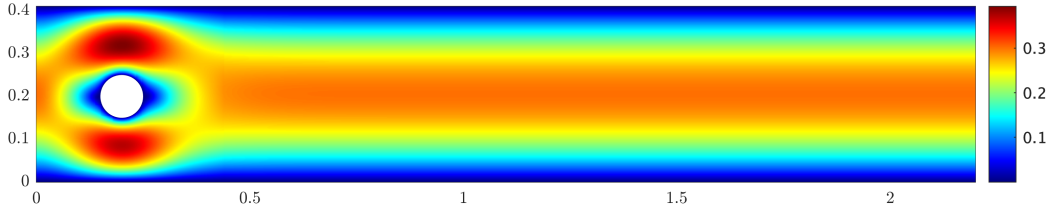
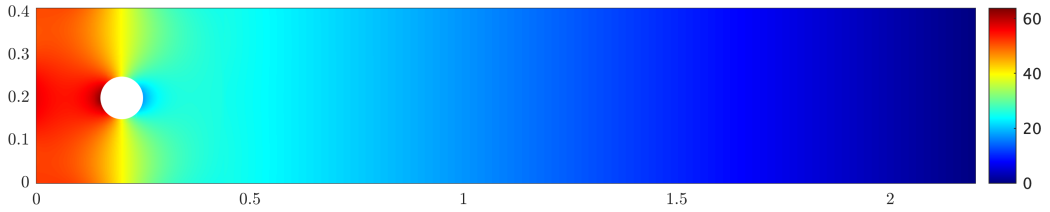


FIGURE 10. Bézier mesh for the *flow around a cylinder*.

Let us set $k = 3$, $\gamma = 10(k + 1)^2$ and consider the mesh configuration depicted in Figure 10, with 2^6 elements in the x -direction and 2^4 elements in the y -direction. In Figure 11 we show the magnitude of the velocity field and the pressure in the case of the stabilized formulation (3) for $m = 0$ with the Nédélec isogeometric element. Note that both the velocity and pressure fields do not show any spurious oscillations around the trimmed part of the boundary and seem to comply with their physical meaning.



(a) Magnitude of the velocity.



(b) Pressure.

FIGURE 11. Numerical solutions of the non-symmetric stabilized formulation (10) for the *flow around a cylinder* with the Nédélec element.

7.6. Lid-driven cavity

The lid-driven cavity is another important benchmark for the Stokes problem where the incompressible flow in a confined volume is driven by the tangential in-plane motion of two opposite bounding walls [27, 47]. Here, the cavity is represented by the trimmed domain $\Omega = (-1, 1) \times (-3, 3)$ immersed in Ω_0 . Ω_0 is the rectangle with vertices $(-3, -3.5)$, $(3, -3.5)$, $(3, 3.5)$, $(-3, 3.5)$ rotated of $\frac{\pi}{6}$ counterclockwise around the origin. No-slip Dirichlet boundary conditions are imposed on the left and right sides of the cavity, while the top and bottom ones are walls sliding, respectively, to the right and left with unitary velocity magnitude, namely we enforce the non-homogenous Dirichlet boundary conditions

$$\mathbf{u}(x, 3) = \begin{pmatrix} 1 \\ 0 \end{pmatrix} \quad \text{on} \quad \{(x, 3) : x \in [-1, 1]\}, \quad \mathbf{u}(x, -3) = \begin{pmatrix} -1 \\ 0 \end{pmatrix} \quad \text{on} \quad \{(x, -3) : x \in [-1, 1]\}.$$

Since the Dirichlet boundary conditions have a jump at the corners, the trace of the solution for the velocity does not belong to $\mathbf{H}^{\frac{1}{2}}(\Gamma)$, hence $\mathbf{u} \notin \mathbf{H}^1(\Omega)$. The applied body force is $\mathbf{f} = \mathbf{0}$. We solve the problem by using the non-symmetric stabilized formulation (10), discretized using the Taylor-Hood element, with degree $k = 2$, penalty parameter $\gamma = 30(k+2)^2$ and mesh-sizes $h_x = h_y = 2^{-5}$ along the first and second parametric directions respectively. The mesh employed for the numerical simulation is depicted in Figure 12a. In Figures 12b, 12c the numerical solutions for the velocity and the pressures are plotted: our results are qualitatively in accordance with the ones of [13, 27].

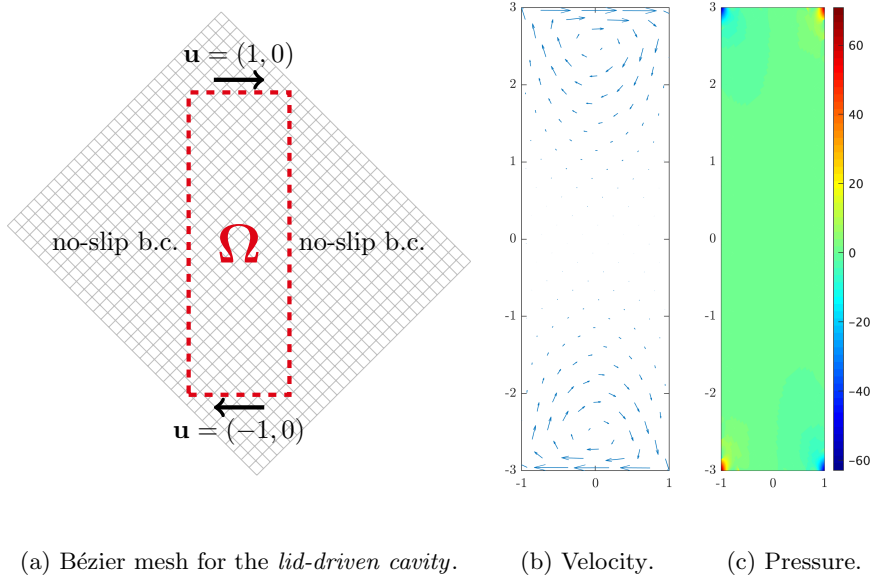


FIGURE 12. Numerical solutions of the non-symmetric stabilized formulation (10) for the *lid-driven cavity* with the Taylor-Hood element.

APPENDIX A. USEFUL INEQUALITIES

In this section, we collect some technical results repeatedly employed throughout the manuscript. The constants that will appear in the inequalities below, unless otherwise specified, are intended to be robust with respect to the mesh size and mutual position between trimming curve and active physical Bézier mesh.

Lemma A.1. *There exists $C > 0$, depending on Γ , such that, for every $K \in \mathcal{G}_h$,*

$$\|v\|_{L^2(\Gamma_K)}^2 \leq C \|v\|_{L^2(K)} \|v\|_{H^1(K)}, \quad \forall v \in H^1(K).$$

Proof. See, for instance, Lemma 3 in [28], Lemma 3 in [29], or Lemma 4.1 of [44]. \square

Lemma A.2. *Let $Q, Q' \in \widehat{\mathcal{M}}_h$ be neighbor elements in the sense of Definition 4.1. There exists $C > 0$ such that*

$$\|\varphi\|_{L^\infty(Q)} \leq C \|\varphi\|_{L^\infty(Q')}, \quad \forall \varphi \in \mathbb{Q}_p(\mathbb{R}^d),$$

where C depends on p , on the shape regularity of the mesh, and on the distance between Q and Q' .

Proof. The proof follows by a scaling argument. \square

The next result says that the L^2 -norm on the cut portion of an element Q controls the L^∞ -norm (and hence any other) on the whole element with an equivalence constant depending on the relative measure of the cut portion.

Lemma A.3. *Let $\theta \in (0, 1]$. There exists $C > 0$ such that, for every $Q \in \widehat{\mathcal{M}}_h$ and every $S \subset Q$ measurable such that $|S| \geq \theta |Q|$, we have*

$$\|\varphi\|_{L^\infty(Q)} \leq Ch^{-\frac{d}{2}} \|\varphi\|_{L^2(S)}, \quad \forall \varphi \in \mathbb{Q}_p(\mathbb{R}^d),$$

where C depends only on θ , p , and the mesh regularity.

Proof. See Proposition 1 in [25]. □

Let us recall a more standard inverse inequality with an explicit dependence on the polynomial degree p .

Lemma A.4. *There exists $C > 0$, depending on the shape regularity of the mesh, such that, for every $Q \in \widehat{\mathcal{M}}_h$,*

$$\|\varphi\|_{L^\infty(Q)} \leq Cp^d h_Q^{-\frac{d}{2}} \|\varphi\|_{L^2(Q)}, \quad \forall \varphi \in \mathbb{Q}_p(Q).$$

Proof. We refer the interested reader to [45]. □

REFERENCES

- [1] Robert A. Adams and John J. F. Fournier. *Sobolev spaces*, volume 140 of *Pure and Applied Mathematics (Amsterdam)*. Elsevier/Academic Press, Amsterdam, second edition, 2003.
- [2] Pablo Antolin, Annalisa Buffa, and Massimiliano Martinelli. Isogeometric analysis on V-reps: first results. *Comput. Methods Appl. Mech. Engrg.*, 355:976–1002, 2019.
- [3] John W. Barrett and Charles M. Elliott. A finite-element method for solving elliptic equations with Neumann data on a curved boundary using unfitted meshes. *IMA J. Numer. Anal.*, 4(3):309–325, 1984.
- [4] John W. Barrett and Charles M. Elliott. Finite element approximation of the Dirichlet problem using the boundary penalty method. *Numer. Math.*, 49(4):343–366, 1986.
- [5] Klaus-Jürgen Bathe. The inf-sup condition and its evaluation for mixed finite element methods. *Comput. & Structures*, 79(2):243–252, 2001.
- [6] Evren Bayraktar, Otto Mierka, and Stefan Turek. Benchmark computations of 3d laminar flow around a cylinder with cfx. *International Journal of Computational Science and Engineering*, pages 10–1504, 2012.
- [7] Y. Bazilevs, L. Beirão da Veiga, J. A. Cottrell, T. J. R. Hughes, and G. Sangalli. Isogeometric analysis: approximation, stability and error estimates for h -refined meshes. *Math. Models Methods Appl. Sci.*, 16(7):1031–1090, 2006.
- [8] Roland Becker, Erik Burman, and Peter Hansbo. A Nitsche extended finite element method for incompressible elasticity with discontinuous modulus of elasticity. *Comput. Methods Appl. Mech. Engrg.*, 198(41-44):3352–3360, 2009.
- [9] L. Beirão da Veiga, A. Buffa, G. Sangalli, and R. Vázquez. Mathematical analysis of variational isogeometric methods. *Acta Numer.*, 23:157–287, 2014.
- [10] Christine Bernardi, Claudio Canuto, and Yvon Maday. Generalized inf-sup conditions for Chebyshev spectral approximation of the Stokes problem. *SIAM J. Numer. Anal.*, 25(6):1237–1271, 1988.
- [11] Andrea Bressan. Isogeometric regular discretization for the Stokes problem. *IMA J. Numer. Anal.*, 31(4):1334–1356, 2011.
- [12] Andrea Bressan and Giancarlo Sangalli. Isogeometric discretizations of the Stokes problem: stability analysis by the macroelement technique. *IMA J. Numer. Anal.*, 33(2):629–651, 2013.
- [13] A. Buffa, C. de Falco, and G. Sangalli. IsoGeometric Analysis: stable elements for the 2D Stokes equation. *Internat. J. Numer. Methods Fluids*, 65(11-12):1407–1422, 2011.
- [14] A. Buffa, R. Puppi, and R. Vázquez. A minimal stabilization procedure for isogeometric methods on trimmed geometries. *SIAM J. Numer. Anal.*, 58(5):2711–2735, 2020.
- [15] A. Buffa, J. Rivas, G. Sangalli, and R. Vázquez. Isogeometric discrete differential forms in three dimensions. *SIAM J. Numer. Anal.*, 49(2):818–844, 2011.
- [16] Erik Burman. Ghost penalty. *C. R. Math. Acad. Sci. Paris*, 348(21-22):1217–1220, 2010.
- [17] Erik Burman, Susanne Claus, Peter Hansbo, Mats G. Larson, and André Massing. CutFEM: discretizing geometry and partial differential equations. *Internat. J. Numer. Methods Engrg.*, 104(7):472–501, 2015.
- [18] Erik Burman and Peter Hansbo. Fictitious domain methods using cut elements: III. A stabilized Nitsche method for Stokes’ problem. *ESAIM Math. Model. Numer. Anal.*, 48(3):859–874, 2014.
- [19] J. Austin Cottrell, Thomas J. R. Hughes, and Yuri Bazilevs. *Isogeometric analysis*. John Wiley & Sons, Ltd., Chichester, 2009. Toward integration of CAD and FEA.
- [20] F. de Prenter, C. V. Verhoosel, and E. H. van Brummelen. Preconditioning immersed isogeometric finite element methods with application to flow problems. *Comput. Methods Appl. Mech. Engrg.*, 348:604–631, 2019.
- [21] F. de Prenter, C. V. Verhoosel, G. J. van Zwieten, and E. H. van Brummelen. Condition number analysis and preconditioning of the finite cell method. *Comput. Methods Appl. Mech. Engrg.*, 316:297–327, 2017.
- [22] John A. Evans and Thomas J. R. Hughes. Explicit trace inequalities for isogeometric analysis and parametric hexahedral finite elements. *Numer. Math.*, 123(2):259–290, 2013.
- [23] John A. Evans and Thomas J. R. Hughes. Isogeometric divergence-conforming B-splines for the Darcy-Stokes-Brinkman equations. *Math. Models Methods Appl. Sci.*, 23(4):671–741, 2013.
- [24] John A. Evans and Thomas J. R. Hughes. Isogeometric divergence-conforming B-splines for the steady Navier-Stokes equations. *Math. Models Methods Appl. Sci.*, 23(8):1421–1478, 2013.
- [25] Michel Fournié and Alexei Lozinski. Stability and optimal convergence of unfitted extended finite element methods with Lagrange multipliers for the Stokes equations. In *Geometrically unfitted finite element methods and applications*, volume 121 of *Lect. Notes Comput. Sci. Eng.*, pages 143–182. Springer, Cham, 2017.
- [26] J. Freund and R. Stenberg. On weakly imposed boundary conditions in the finite element method. In M. Morandi Cecchi, editor, *The ninth conference on Finite Elements in Fluids, Venezia, 16.-20.10.1995*, pages 327–336, 1995.
- [27] F. Gürçan. Streamline topologies in stokes flow within lid-driven cavities. *Theoretical and Computational Fluid Dynamics*, 17:19–30, 2003.
- [28] Anita Hansbo and Peter Hansbo. An unfitted finite element method, based on Nitsche’s method, for elliptic interface problems. *Comput. Methods Appl. Mech. Engrg.*, 191(47-48):5537–5552, 2002.
- [29] Anita Hansbo and Peter Hansbo. A finite element method for the simulation of strong and weak discontinuities in solid mechanics. *Comput. Methods Appl. Mech. Engrg.*, 193(33-35):3523–3540, 2004.

- [30] Ralf Hiptmair, Jingzhi Li, and Jun Zou. Universal extension for Sobolev spaces of differential forms and applications. *J. Funct. Anal.*, 263(2):364–382, 2012.
- [31] Tuong Hoang. *Isogeometric and immersogeometric analysis of incompressible flow problems*. PhD thesis, TU Eindhoven, 2018.
- [32] Tuong Hoang, Clemens V. Verhoosel, Ferdinando Auricchio, E. Harald van Brummelen, and Alessandro Reali. Mixed isogeometric finite cell methods for the Stokes problem. *Comput. Methods Appl. Mech. Engrg.*, 316:400–423, 2017.
- [33] Tuong Hoang, Clemens V. Verhoosel, Ferdinando Auricchio, E. Harald van Brummelen, and Alessandro Reali. Skeleton-stabilized isogeometric analysis: high-regularity interior-penalty methods for incompressible viscous flow problems. *Comput. Methods Appl. Mech. Engrg.*, 337:324–351, 2018.
- [34] Tuong Hoang, Clemens V. Verhoosel, Chao-Zhong Qin, Ferdinando Auricchio, Alessandro Reali, and E. Harald van Brummelen. Skeleton-stabilized immersogeometric analysis for incompressible viscous flow problems. *Comput. Methods Appl. Mech. Engrg.*, 344:421–450, 2019.
- [35] T. J. R. Hughes, J. A. Cottrell, and Y. Bazilevs. Isogeometric analysis: CAD, finite elements, NURBS, exact geometry and mesh refinement. *Comput. Methods Appl. Mech. Engrg.*, 194(39-41):4135–4195, 2005.
- [36] D. Kamensky, M.-C. Hsu, D. Schillinger, J. A. Evans, A. Aggarwal, Y. Bazilevs, M. S. Sacks, and T. J. R. Hughes. An immersogeometric variational framework for fluid-structure interaction: application to bioprosthetic heart valves. *Comput. Methods Appl. Mech. Engrg.*, 284:1005–1053, 2015.
- [37] David Kamensky, Ming-Chen Hsu, Yue Yu, John A. Evans, Michael S. Sacks, and Thomas J. R. Hughes. Immersogeometric cardiovascular fluid-structure interaction analysis with divergence-conforming B-splines. *Comput. Methods Appl. Mech. Engrg.*, 314:408–472, 2017.
- [38] Benjamin Marussig and Thomas J. R. Hughes. A review of trimming in isogeometric analysis: challenges, data exchange and simulation aspects. *Arch. Comput. Methods Eng.*, 25(4):1059–1127, 2018.
- [39] Fady Massarwi and Gershon Elber. A B-spline based framework for volumetric object modeling. *Comput.-Aided Des.*, 78:36–47, 2016.
- [40] R. A. Nicolaides. Existence, uniqueness and approximation for generalized saddle point problems. *SIAM J. Numer. Anal.*, 19(2):349–357, 1982.
- [41] Riccardo Puppi. Isogeometric discretizations of the Stokes problem on trimmed geometries. arXiv, 2020.
- [42] Alfio Quarteroni and Alberto Valli. *Numerical approximation of partial differential equations*, volume 23 of *Springer Series in Computational Mathematics*. Springer-Verlag, Berlin, 1994.
- [43] Ernst Rank, Martin Ruess, Stefan Kollmannsberger, Dominik Schillinger, and Alexander Düster. Geometric modeling, isogeometric analysis and the finite cell method. *Computer Methods in Applied Mechanics and Engineering*, 249-252:104 – 115, 2012. Higher Order Finite Element and Isogeometric Methods.
- [44] Arnold Reusken. Analysis of trace finite element methods for surface partial differential equations. *IMA J. Numer. Anal.*, 35(4):1568–1590, 2015.
- [45] Ch. Schwab. *p- and hp-finite element methods*. Numerical Mathematics and Scientific Computation. The Clarendon Press, Oxford University Press, New York, 1998. Theory and applications in solid and fluid mechanics.
- [46] Rolf Stenberg. On some techniques for approximating boundary conditions in the finite element method. volume 63, pages 139–148. 1995. International Symposium on Mathematical Modelling and Computational Methods Modelling 94 (Prague, 1994).
- [47] L. D. Sturges. Stokes flow in a two-dimensional cavity with moving end walls. *Physics of Fluids*, 29:1731–1734, 1986.
- [48] Luc Tartar. *An introduction to Sobolev spaces and interpolation spaces*, volume 3 of *Lecture Notes of the Unione Matematica Italiana*. Springer, Berlin; UMI, Bologna, 2007.